Intra-articular delivery of full-length antibodies through the use of an in situ forming depot

Alexis Fayd'Herbe de Maudave, Wilhem Leconet, Karine Toupet, Michael Constantinides, Guillaume Bossis, Marion de Toledo, Jérôme Vialaret, Christophe Hirtz, Adolfo Lopez-Noriega, Christian Jorgensen, et al.

Intra-articular delivery of full-length antibodies through the use of an *in situ* forming depot

Alexis Fayd'herbe De Maudave[1,*], Wilhem Leconet[2], Karine Toupet[1], Michael Constantinides[1,3], Guillaume Bossis[4], Marion de Toledo[4], Jérôme Vialaret[3], Christophe Hirtz[3], Adolfo Lopez-Noriega[2], Christian Jorgensen[1,3], Daniele Noel[1,3], Pascale Louis-Plence[1], Sylvestre Grizot[2,#,*] and Martin Villalba[1,3,5,6 #, *]

[1] IRMB, Univ Montpellier, INSERM, Montpellier, France

[2] MedinCell SA, Jacou, France

[3] IRMB, CHU Montpellier, Montpellier, France

[4] IGMM, Univ Montpellier, CNRS, Montpellier, France

[5] IRMB, Univ Montpellier, INSERM, CNRS, CHU Montpellier, Montpellier, France

[6] Institut Sainte-Catherine, Avignon, France

*corresponding authors: sylvestre.grizot@medincell.eu; martin.villalba@inserm.fr

[#] shared senior authorship

1. ABSTRACT

Monoclonal antibodies (mAbs) are large size molecules that have demonstrated high therapeutic potential for the treatment of cancer or autoimmune diseases. Despite some excellent results, their intravenous administration results in high plasma concentration. This triggers off-target effects and sometimes poor targeted tissue distribution. To circumvent this issue, we investigated a local controlled-delivery approach using an *in situ* forming depot technology. Two clinically relevant mAbs, rituximab (RTX) and daratumumab (DARA), were formulated using an injectable technology based on biodegradable PEG-PLA copolymers. The stability and controlled release features of the formulations were investigated. HPLC and mass spectrometry revealed the preservation of the protein structure. *In vitro* binding of formulated antibodies to their target antigens and to their cellular FcγRIIIa natural killer cell receptor was fully maintained. Furthermore, encapsulated RTX was as efficient as classical intravenous RTX treatment to inhibit the *in vivo* tumor growth of malignant human B cells in immunodeficient NSG mice. Finally, the intra-articular administration of the formulated mAbs yielded a sustained local release associated with a lower plasma concentration compared to the intra-articular delivery of non-encapsulated mAbs. Our results demonstrate that the utilization of this polymeric technology is a reliable alternative for the local delivery of fully functional clinically relevant mAbs.

---

2. KEYWORDS

Full length monoclonal antibodies; Intra-articular; Local delivery; biodegradable copolymers; rituximab; daratumumab.

3. INTRODUCTION

A considerable number of monoclonal antibodies (mAbs) have been approved in clinics and are a fast growing group among new therapeutics as they offer exquisite specificity[1]. This immunotherapy has revolutionized the way to treat patients in many therapeutic areas, including oncology and auto-immune diseases. Due to their intrinsic biochemical nature, antibodies are not used orally and are mostly administrated intravenously or subcutaneously [2]. Both routes of administration can lead to side effects related to their initial elevated concentration. The large size of antibodies, together with neonatal Fc receptor (FcRn)-mediated recycling, confer them a long half-life generally comprised between two to three weeks. This makes them amenable to convenient dosing regimen. Hence, and in contrast to therapeutic peptides or small proteins, mAbs are not usually considered for drug delivery systems [3]. However, the large mAb size can be problematic to reach certain tissues or compartments, which are poorly vascularized or present a barrier for protein infiltration[4]. This results in a lower treatment efficacy or a higher toxicity due to the necessity to increase the administered dose[5]. Developing strategies to achieve local delivery would improve mAbs efficacy and could reduce the treatment costs as a consequence of the administered dose reduction. Sophisticated technologies relying either on protein engineering or on drug carrier modifications would provide a specific recognition of the targeted tissue or cell type while significantly increasing the manufacturing cost or affecting the production yield [6–10]. A more straightforward approach is the direct injection of the drug in the targeted tissue or compartment. It has been for instance successfully used in ocular applications with intravitreal injections of anti-VEGF antibodies or antibody fragments such as ranibizumab, bevacizumab or aflibercept for the treatment of macular diseases[11]. However, even in a close compartment like the eye, the intravitreal injection of anti-VEGF agents presented systemic effects with the suppression of plasma-free VEGF for several days, even at a dose more than 100-fold lower than the one used in oncology via a systemic delivery [12]. In the oncology field, intratumor injection of checkpoint inhibitors, *e.g.* anti-CTLA4, has been explored to reduce their toxicity profile [13]. Still, a direct injection of the therapeutic protein

in a targeted compartment does not necessarily translate in a prolonged, high local exposure of the molecule. For instance, an intra-articular injection of a protein-containing saline solution does not result in long-term residence of the protein, which is quickly retrieved from the systemic circulation due to the efficient lymphatic drainage of the joint[14]. Conversely, targeting the joint using a systemic approach is complicated as the synovial fluid is an ultrafiltrate of the plasma. Indeed, after intravenous injection, a small fraction of proteins can be detected in the synovial fluid. Moreover, the larger the protein, the lower the synovial to serum concentration ratio will be[15]. As a consequence, the expected synovial fluid concentration of a mAb is 3 to 10 times lower than the serum one, a feature that could explain the lack of efficacy of certain molecules evaluated for the treatment of osteoarthritis. There is therefore a need to design long-acting injectables for local, intra-articular, mAb delivery that would sustain high local concentrations and improve treatment efficacy for a condition (osteoarthritis) with current unmet medical needs.

The aim of the present work is to design a sustained release formulation of a full-length model mAb for intra-articular delivery, using an *in situ* forming depot (ISFD) long-acting technology registered under the name of BEPO®. BEPO® technology relies on the use of copolymers based on polyethylene glycol (PEG) or methoxy-PEG (mPEG) and poly D,L lactic acid (PDLLA). Specifically, on the combination of one triblock (PDLLA-PEG-PDLLA) and one diblock (mPEG-PDLLA) copolymer. These copolymers are designed for not being soluble in water and need to get solubilized in an organic solvent to prepare an injectable formulation. Upon injection into an aqueous environment, the formulation forms a solid polymeric depot due to the diffusion of the organic solvent and the subsequent precipitation of the copolymers. If a therapeutic molecule is incorporated into the formulation, it will be trapped within the precipitated polymeric matrix and will be delivered in a controlled fashion thereafter[16]. The release kinetics of the formulated drug can be modulated by varying different parameters such as polymer composition or polymer content in the initial formulation. This technology has the potential to provide sustained release formulations for the local or systemic delivery of small

molecules with release kinetics varying from weeks to months. It was also successfully used to formulate a 55 kDa bispecific antibody in a half-life extension strategy and the functionality of the formulated protein was fully established[17]. However, the efficacy of this technology to formulate full-size mAbs is unknown. This is clinically relevant because the vast majority of Abs used nowadays in therapeutics present molecular weights higher than 140 kDa.

Anti-CD20 Rituximab (RTX) and anti-CD38 Daratumumab (DARA), two clinically validated and well characterized mAbs, were chosen in the present study to evaluate the capacity of BEPO® technology to successfully deliver them in the intra-articular region. Formulated mAbs were extensively characterized for their physico-chemical properties and biological activity while *in vivo* pharmacokinetic studies were conducted in mice after intra-articular (IA) injection of ISFD formulations to evaluate the delivery of the mAb in the synovial fluid.

4. MATERIALS AND METHODS

4.1. Materials

RTX and DARA proteins were obtained from the commercial products MabThera® and Darzalex®, respectively. Protein sequences for the murine version of RTX were taken from the following reference [18] and the mouse RTX (mRTX) protein was produced by Evitria AG, Switzerland. The rat IgG2a isotype control was purchased from BioXCell (Lebanon, NH, USA). Triblock (TB) and diblock (DB) copolymers were produced by CM Biomaterials (Tucker, GA, USA). If not otherwise stated, all chemicals were obtained from Sigma-Aldrich and used without further purification.

BEPO® polymeric vehicles (*i.e.* a solution of copolymers in tripropionin) used in this study are summarized in Table 1. Triblocks (TB) and diblocks (DB) are presented with the molecular weights in kDa of (m)PEG and PDLLA in the copolymers. The total polymer content is expressed as a mass percentage. For instance, the vehicle V1 from Table 1 was obtained by solubilizing a triblock with 3 kDa PEG and 9.8 kDa PDLLA (presented as 3-9.8 in Table 1), and a diblock with 1 kDa PEG and 6.5 kDa PDLLA (presented as 1-6.5 in Table 1) in

tripropionin. The weight fraction of copolymers in the final vehicle was 20 % (w/w) with a 1:1 TB:DB weight ratio.

Table 1 : *Composition of vehicles used to make BEPO®:protein formulations*

Vehicle	TB:DB couple	Triblock	Diblock	Polymer content (% w/w)	TB:DB weight ratio
V1	TB1:DB1	3-9.8	1-6.5	20	1:1
V2	TB1:DB1	3-9.8	1-6.5	20	3:1
V3	TB1:DB2	3-9.8	2-27.8	20	1:1

In the manuscript, Vx refers to a polymer vehicle (copolymers solubilized in tripropionin) while Fx refers to a drug loaded formulation where a spray dried cake has been dispersed into the corresponding vehicle.

4.2. Spray Drying of antibody solutions

RTX or DARA commercial solutions were buffer exchanged through the use of desalting PD-10 columns (Merck). In the final solution, protein concentration was comprised between 7 and 10 mg/mL. Then, antibody solutions were spray dried using a Mini B290 apparatus (Büchi, Switzerland). Inlet temperature and liquid feed rate were set at 85°C and 1.5 mL/min, respectively. Aspirator was set at 100 % and air flow at 55 on the device. The outlet temperature recorded during the process was comprised between 55°C and 58°C. Generally, the process yield was comprised between 70% and 90%. Powder was collected and dried overnight in a vacuum oven at 30°C. Particle size analysis was performed on the dry powder using a MorphologyG3 instrument (Malvern). The dry powder was also submitted to SEM imaging. Thermal analysis was conducted using the Tycho NT.6 instrument (NanoTemper GmbH, Munich, Germany). The instrument relies on the protein intrinsic fluorescence and records the ratio of emitted fluorescence at 350 nm over 330 nm over a temperature ramp between 35°C and 95°C. Temperatures at which a transition occurs are called inflection temperatures (T_i). Both the native RTX and sdRTX proteins were analyzed at a concentration of 0.5 mg/mL in

samples in PBS. The protein content in the spray dried (sd) cake was determined by solubilizing the powder in PBS and quantifying the protein by SEC-HPLC. Trehalose content was also determined using an enzymatic assay based on trehalase activity (Libios, France).

4.3. Preparation of protein ISFD formulations and in vitro release (IVR) studies

Vehicles were made by dissolving the copolymers (TB and DB) in tripropionin overnight. Then, the sd cakes containing the antibodies were weighed and dispersed into the polymer vehicles to reach the targeted final protein loading. Good powder dispersion and formulation homogeneity, assessed visually, were achieved after 30 min under magnetic stirring. Drug assay was performed as follows. Briefly, around 50 mg of formulation (in triplicate) were weighed precisely in a 1.5 mL polypropylene tube. After centrifugation (10 min, 13000 rpm), the supernatant (polymer vehicle) was removed, the pellet was washed three times with 500 µL of ethyl acetate and finally dried for 1 hour in vacuum oven. Dry pellet was solubilized in 1 mL of PBS and the protein concentration was determined by SEC-HPLC. Experiments were carried out in triplicate. Drug assay samples will be noted using a "da" prefix in the following text.

*In vitr*o release (IVR) tests of BEPO®:protein formulations were initially performed in SEC-Tween buffer (50 mM sodium phosphate buffer pH 6.8, 100 mM NaCl and 0.005% Tween80). The presence of Tween80 ensured minimal protein adsorption at low concentrations. However, to ensure full compatibility of the release medium with cell-based assays, regular PBS was later substituted to SEC-Tween as release medium. Around 100 mg of each formulation were injected into 18 mL of buffer in glass vials that were capped and placed at 37°C under continuous orbital shaking. At given time points, the release medium (samples noted with the "iv" prefix) was collected and replaced by preheated buffer. The released protein concentration in the medium was determined by SEC-HPLC and a cumulative release profile was built for each formulation considering the initial protein cargo. IVR studies were performed in triplicate. During IVR studies and after extensive drying of the polymer depot in vacuum oven at 30°C,

the protein was also extracted from the polymer depot (samples note with the "dep" prefix) following the same procedure as for the drug assay and analyzed. For stability studies, formulations were stored at 4°C in 2 mL crimped vials capped with PTFE coated stoppers.

4.4. Liquid chromatography methods

4.4.1. SEC-HPLC method

Size-exclusion chromatography was carried out using a BEH SEC 200 column, 7.8x300 mm, 3.5 µm particle size (Waters, Milford, MA, USA). The eluent was a 50 mM sodium phosphate buffer at pH 6.8 with 250 mM NaCl and 0.02% of sodium azide. 40 µL of sample were injected and elution was carried out at room temperature at a 1 mL/min flow rate. Protein detection was achieved with a fluorescence detector (W2475) using the intrinsic protein fluorescence with excitation and emission wavelengths at respectively 284 nm and 335 nm. RTX eluted at a relative retention time (RRT) of 8.25 min. The chromatogram presented also a high molecular weight aggregated fraction (HMW) at 7.52 min (RRT of 0.91) and a low molecular weight (LMW) specie eluting at 10.06 min (RRT of 1.22) and corresponding most probably to a Fab fragment. The SEC-HPLC method was used to both monitor the HMW or LMW species and quantitate accurately the protein.

4.4.2. RP-HPLC method

RTX samples in PBS were submitted to IdeS (Genovis AB, Sweden) digestion following the manufacturer recommendations and were further reduced using TCEP at 20 mM final concentration. Samples were then analyzed by RP HPLC using the BioResolve RP mAb polyphenyl column from Waters (450 Å, 2.7 µm, 4.6x150 mm). Injection volume was 10 µL and the column temperature was set at 60°C. The eluents were H_2O with 0.1% TFA and acetonitrile with 0.1% TFA. Protein subunits elution was achieved at 1 mL/min using a gradient from 30 % to 40 % acetonitrile in 20 min. The three protein subunits eluted in the Fc/2, LC and Fd sequence order with the following retention times: 6.5, 8.1 and 13.6 min, respectively. Total

impurity level could be reported and for a particular impurity, its level was reported as the percentage of total area relative to the related RTX moiety.

4.4.3. SCX-HPLC method

As the isoelectric point of RTX is greater than 8, cation-exchange is very well suied to try to separate the charge variants of the protein. Hence, SCX-HPLC was carried out at pH 6.2 using a BioResolve SCX mAb, 3µm, 4.6x100 mm column from Waters. The eluent was 20 mM MES at pH 6.2. The protein was eluted with a NaCl gradient (from 75 mM to 150 mM NaCl in 12 min) at a flow rate of 0.5 mL/min.

4.5. Mass spectrometry analyses

For intact-mass analysis, deglycosylated samples (PNGase) were diluted in ultrapure water and 10 µg of protein were injected in Matrix Assisted Laser Desorption Ionisation device (MALDI-TOF-TOF) 4800 Applied Biosystems device.

Full tryptic peptide analysis of native RTX and formulated samples (daRTX, ivRTX and depRTX) was carried out with the following procedure. Samples were acidified with 0.1% TFA (trifluoro acetic acid) up to 80µL. Protein content of the sample was extracted with RP-W cartridges on AssayMap BRAVO automate (Agilent, Lexington, USA). Samples were further reduced with dithiothreitol (DTT) during one hour at 56°C. Free cysteines were alkylated with iodoacetamide (IAA) by adding 7.5 µL of 125 mM IAA and incubating 30 minutes in the dark, at 56°C. Finally, proteins were digested with trypsin (0.5 µg) overnight at 37°C. Digestion was stopped by adding 5 µL of formic acid and peptides were cleaned and desalted with C18 Tips before being dried on Speedvac. After resuspension in 60 µL of 2% acetonitrile/0.1% formic acid/97.9% water, 7 µL of supernatant were injected on nanoElute (Bruker Daltonics, Massachusetts, USA). NanoFlow LC was coupled to Q-TOF MS instrument (Impact II, Bruker Daltonics, Massachusetts, USA) through captive spray ion source (1200V, dry gas: 3 L/min at 150°C) operating with nanobooster (0.2 Bar of Nitrogen boiling in acetonitrile). In the LC part, samples were desalted and pre-concentrated on-line on a PepMap u-precolumn (300 µm x 5 mm, C18 PepMap 100, 5 µm, 100 Å, ThermoFisher, Waltham, MA, USA). To perform the

separation, peptides were transferred to analytical column (75 µm x 500 mm; Acclaim Pepmap RSLC, C18, 2 µm, 100 Å, ThermoFisher, Waltham, MA, USA).

A gradient consisting of 5-26 % B for 192 min and 90% B for 10 min (A = 0.1% formic acid, 2% acetonitrile in water; B = 0.1% formic acid in acetonitrile) at 400 nL/min, 50°C, was used to elute peptides from the reverse-phase column.

For peptide identification, data dependent acquisition (DDA) was performed with a lock-mass as internal calibrator (m/z 1222, Hexakis ‘’1H, 1H, 4H-hexafluorobutyloxy’’ phosphazine, Agilent Technologies, Santa Clara, USA). Using Instant Expertise software (Bruker Daltonics, Massachusetts, USA), the most intense ions per cycle of 3 seconds were selected and then active exclusion was used (after 1 spectrum for 2 minutes unless the precursor ion exhibited intensity higher of three times than the previous scan). All MS/MS spectra were searched against homemade Rituximab database by using the Mascot v 2.6.0 algorithm (Matrix Science, http://www.matrixscience.com/) with the following settings: (1) enzyme: trypsin, (2) variable modifications: oxidation (M) and deamidated (N,Q), (3) fixed modifications: carbamidomethyl (C), (4) missed cleavages: 2, (5) instrument type CID: ESI-QUAD-TOF, (6) peptide tolerance: 10.0 ppm, (7) MS/MS tolerance: 0.05 Da, (8) peptide charge: 1+, 2+ and 3+, (9) mass: monoisotopic, (10) C13: 1, (11) minimum peptide length: 5, (12) peptide decoy: ON, (13) adjust FDR [%]: 1, (14) percolator: on, (15) ions score cut-off: 12, (16) ions score threshold for significant peptide IDs: 12.

4.6. Surface Plasmon Resonance (SPR) experiments

The surface plasmon resonance (SPR) experiments were performed on a BIACORE T200 at 25 °C with PBS containing 0.05% of Tween20 (Cytiva) as running buffer. For FcγR measurements, the capturing anti-his-tag antibody (R&D) was immobilized on three flow cells Fc2,3,4 of a CM5 chip (Cytiva) at 8,000–9,000 RU using a standard amine coupling procedure. Fc1 was taken as a control submitted to the same procedure without any protein. After the capture of FcγR (100-200 RU), samples containing formulated RTX were injected at 100 µL/min at five increasing concentrations in a single run. After a dissociation time of 600 s

with running buffer, the chip surface was regenerated using a 30 s injection of 10 mM glycine-HCl pH 1.7. Bulk refractive index differences were corrected by substracting the response obtained on the reference flow cell. Binding kinetic titrations were analyzed by BiaEvaluation software (T200Evaluation 3.2) using a two-state binding model. For some of these interactions, featuring too fast dissociation to allow the determination of kinetic constants, the affinity constant K_D was determined by steady state analysis. For binding analysis to FcRn, hFcRn was covalently immobilized on CM5 by amine coupling (200-250 RU) and samples presenting a protein concentration of 150 nM were injected at a flow rate of 30 µL/min in 50 mM PBS buffer (pH 6.0) and 0.05% Tween20. After a dissociation step of 400 s with running buffer, the sensor surfaces were regenerated using two pulses of PBS buffer (pH 7.4). To compare the binding kinetics of the different samples on immobilized FcRn, responses (in RU) at three time points on the curves, 180, 200, and 580 s, designated as binding, stability 1, and stability 2, respectively, were measured. Data were read directly on the curve to be independent of fitting. The stability of the coated surface was checked by injection of RTX (50 nM) as a positive control at the beginning and end of the series of experiments.

4.7. Cell lines and cell culture

Raji and Daudi (B cell lines derived from Burkitt lymphomas), Molm-13 (derived from acute monocytic leukemia (AML-M5a)), PLH (Epstein-Barr Virus (EBV) transformed lymphoblastoid cell line) and K-562 (derived from chronic myelogenous leukemia) were obtained from ATCC. The primary BCL-P2 cells (derived from a B-cell lymphoma patient) have already been described elsewhere[19,20]. All cells were cultured in RPMI Glutamax™ medium supplemented with FBS (10%), at 37°C in a humidified 5% CO_2 atmosphere incubator in a BSL-2 facility without any antibiotics. All cell lines were tested for potential mycoplasma contamination using a commercial kit (Lonza). Prior to any medium change, cells were counted using trypan blue exclusion or a Muse cell counter device (Millipore). Expanded human NK cells (eNKs) were produced from umbilical cord blood (UCB) as previously described [21]. Briefly, after PBMCs ficoll extraction, CD3+ cells were depleted with an EasySep™ kit (Stem

Cells). CD56 positive cells were determined by a CD3-/CD56+ cells staining on the Muse device. According to CD56 number, PLH irradiated cells (4:1) were added to NK cells culture with RPMI-FBS (10%) supplemented with IL-2 and IL-15 (100 UI/mL and 5 ng/mL, respectively) After 14-21 days, eNK were ready to use [21].

4.8. Antibody Dependent Cellular Cytotoxicity assay (ADCC) on B cell lines

Sensitive target cells (Raji, BCL-P2, PLH, Daudi) were stained with CellTrace™ Violet cyto trace violet (CTV; 4 µM) in PBS for 20 min at 37°C. Resistant target cells (Molm-13) were stained with CytoTracker™ Green (CTG; 4 µM) and used as internal control. Cells were then centrifuged (5 min, 500 g, RT) and resuspended in 14 mL of RPMI medium (without FBS) during 30 min at 37°C. Then, sensitive and resistant cells and effector (eNK) cells were placed together in a 96-well plate at 0.5 million cells in 200 µL per well. After centrifugation (5 min, 450 g), cells were resuspended in RPMI-10% FBS containing native or formulated RTX overnight at 37 °C with eNKs at the expected ratios. Afterwards, cells were washed and stained in 100 µL during 20 min at 4°C with fluorescent antibodies and chemicals. CD56-PE staining and target cell tracker staining were used to better distinguish effector and target cell populations. Viobility (FL9) for Daudi and 7AAD (FL4) staining for Raji were used to assess cell death. Cells were washed and analysed by FACs in a Gallios 3L (Beckman) using Kaluza software [22,23]. eNK natural cytotoxicity was measured in absence of antibody. After doublet exclusion, death staining signal was observed over CD56 negative population.

4.9. NFAT reporter activation assay

Effector and target cells from the ADCC Reporter Bioassay (Promega) were thawed the day of the experiment and resuspended in RPMI 1640 medium with 4% low IgG FBS. Effector cells were added to each well (75,000 cells per well) of a V-bottom 96-well plate. Target cells were then added at 6:1 (E:T) ratio. 25 µL of RTX samples were added for a final volume of 75 µL and samples incubated during 8 hours at 37°C (5% CO_2). Afterwards, the plate was placed 15 minutes at RT prior the addition of the Nano-Glo®Dual-luciferase® reagent. Then, a sequential

quantification of luminescence at t=10-30 min was performed using a bioluminescence reader. Samples were analyzed in triplicate.

4.10. CD20 binding assay

Raji cells were plated in 96-well round bottom plates at $1x10^6$ cells/mL in 200 µL. The different RTX samples were added for 30 min at 4°C and cells were washed three times in PBS 2% FBS. RTX was targeted using an AlexaFluor647 conjugated anti-human IgG (H+L) antibody (Jackson Immunoresearch) at an 800-fold dilution for 30 min at 4°C. Cells were washed three times in PBS and resuspended in 250 µL of PBS with 2 % FBS before FACS analysis. 10 000 events were analysed by FACs in a Gallios 3L (Beckman) using Kaluza software.

4.11. RTX and formulated RTX antitumor activity

BCL-P2 cells (5×10^6 in 50 µL PBS) were injected subcutaneously (flank area) in 6-10 week-old NOD scid gamma (NSG) mice. Four days later, mice were randomized in the different treatment groups and at day 6, RTX was administered intravenously as a saline solution or subcutaneously for the RTX ISFD formulation at a dose of 10 mg/kg. At 5, 13 and 20 days, 5×10^6 eNK were injected. Mice weight and tumor size were measured at 5, 7, 13, 19, 20, 21, 26, 28, 33, 35, 38, 42, 48, and 53 days after RTX administration.

4.12. RTX, mRTX, DARA and ADA detection by ELISA

In-house ELISA assay was developed using a pair of anti-RTX antibodies (HCA186 for the capture, MCA2260P for the detection) (BioRad). As both antibodies recognize RTX paratopes, mRTX could be quantified as well using the same assay. Briefly, 96 half-well plates were coated overnight at 4°C with 50 µL of HCA186 at 1 µg/mL in PBS. After washing in PBST (PBS + 0.05% Tween20) and blocking with PBST supplemented with 5% BSA during 90 min at room temperature (RT), standards and samples were adequately diluted in PBST and 50 µL were incubated during 1 hour at RT. Detection was achieved using the HRP conjugated antibody MCA2260P at 1 µg/mL in blocking buffer (5% BSA in PBST) and incubated with 3,3',5,5'-tétraméthylbenzidine (TMB) peroxidase substrate. The optical density was measured

at 450 nm after HCl 1N addition. Each sample was analyzed in duplicate. The RTX standard curve (0.6 to 450 ng/mL) was fit using a 4-parameter logistic regression. As the limit of detection in the ELISA assay was around 2 ng/mL, associated with a maximal sample dilution of 5-fold, the RTX LOQ (Limit of Quantification) was around 10 ng/mL.

DARA quantification in mice serum or RPMI after knee collection was made using an ELISA kit for Human IgG (ThermoFisher), following the manufacturer recommendations.

Anti-RTX antibodies were detected through a simple ELISA assay using RTX as a probe (overnight coating at 1.5 µg/mL in PBS), incubation of the samples after adequate dilution (50-fold and 20-fold dilutions for the serum and synovial samples, respectively) during 1 hour at room temperature and detection of the anti-RTX mice antibodies with a goat anti-mouse IgG HRP (Abcam).

4.13. Biocompatibility and pharmacokinetics studies after IA delivery

In vivo studies were performed using 10-week old C57BL/6j male mice. Experiments were performed in accordance with the European Community guidelines (86/609/EEC) and the French National Committee (87/848) for the care and use of laboratory animals and were approved by the regional ethics committee for animal experimentation in Languedoc Roussillon (Reference APAFIS#21840-2019081912221252, n°036; approval number: CEEA-LR-12163). Test items (physiological serum, saline protein solutions and ISFD formulations or vehicles) were injected IA (2.5 µL) into the right knee of animals to achieve a RTX dose of 25 µg. Blood sampling was performed at 1, 7, 14, 21 and 28 days. Knee joints were recovered at day 1, 14, 21 and 28 and incubated for 1 hour at 37°C in 1 mL of RPMI medium after rupture of the synovial capsule to obtain the synovial fluid. RTX concentration in synovial fluid was adjusted considering arbitrarily a knee synovial fluid volume of 5 µL. Recovered knees were fixed 7 days in 3.7% formaldehyde at ambient temperature. Knees were then rinsed and decalcified in 5% formic acid solution for 7 days. After paraffin inclusion, three frontal sections of 7 µm in thickness and spaced by 100 µm were recovered from each tibia and stained with hematoxylin/eosin or safranin O/fast green staining. Synovitis was graded on

hyperplasia/enlargement of synovial lining layer and the degree of inflammatory infiltration as follows: no synovitis (0), slight (1), moderate (2) and strong synovitis (3).

Osteophyte formation was attributed a score from 0 (absence of osteophytes) to 3 (osteophyte with the highest volume) depending on the osteophyte volume at the edge of lateral and median tibial plateaus. The final score is the mean of the scores attributed for the 3 sections obtained from each sample.

4.14. Statistical analysis

All statistics were performed using Graph Pad Prism version 9.1.0 All tests were performed on at least three experiments within technical triplicates. All graphs present means, and standard deviation obtained by row stats or column stats tools. Multiple comparisons of repeated assays were done over each group within each experiment (mean, n and SD) using Two-way ANOVA to compare the different conditions. All XY data were analysed by spearman correlation.

5. RESULTS

The proteins were formulated in solid state. For this purpose, copolymers were first solubilized in tripropionin, a small chain triglyceride that presents a low solubility into water, to obtain a so-called polymer vehicle. Then, a protein solid cake was dispersed into the polymer vehicle to achieve the targeted protein loading (Suppl. Fig. S1). Preliminary experiments had shown that a spray dried (sd) protein cake was more suitable than a lyophilized sample to achieve high drug loading, and easy to resuspend homogenous formulation (data not shown). The first step was hence to produce a sd mAb cake.

5.1. mAb ISFD formulations

MabThera® solution was spray dried without any prior manipulation. The particle size distribution analysis of the obtained powder revealed a mean particle size of 5.5 µm and a narrow particle size distribution (D_{90} of 9.1 µm) (Fig. 1A). SEM imaging of the spray dried cake confirmed the presence of a homogenous population with most particles presenting a dry grape shape (Fig. 1B). The RTX commercial product should theoretically lead to a powder

presenting 37 % (w/w) protein content along with salt (NaCl) and buffering agent (sodium citrate). After solubilization of the spray dried cake into water, no visible particles could be observed, and the protein was quantified either by SEC-HPLC or by using a micro-BCA assay. Both methods retrieved the expected protein content value, which confirmed the fact that the drying process did not induce a preferential loss of the protein. However, after a centrifugation step (10 min, 16000 g), a 2 % protein loss was observed with the BCA assay and not by SEC-HPLC, which could be an indication of the presence of some subvisible particles in the protein solution. The SEC-HPLC analysis of the spray dried RTX (sdRTX) showed also that the drying process induced a slight increase from 0.6 % to 1.2 % of the HMW fraction (Fig. 1C). Finally, a thermal analysis was conducted on the native RTX and the sdRTX protein solubilized in PBS, displaying superimposable profiles with very similar transition temperatures (Fig. 1D) and showing that the first inflection temperature was over 70°C while the observed outlet temperature during the spray drying process was below 60°C. Finally, mass spectrometry analysis was performed on the full-length proteins (native RTX and sdRTX) after deglycosylation showing the same molecular weight for both proteins corresponding to lysine-clipped heavy chains and the presence of pyro-glutamate as a N-terminal residue in both the light and heavy chains (Suppl. Fig. S2).

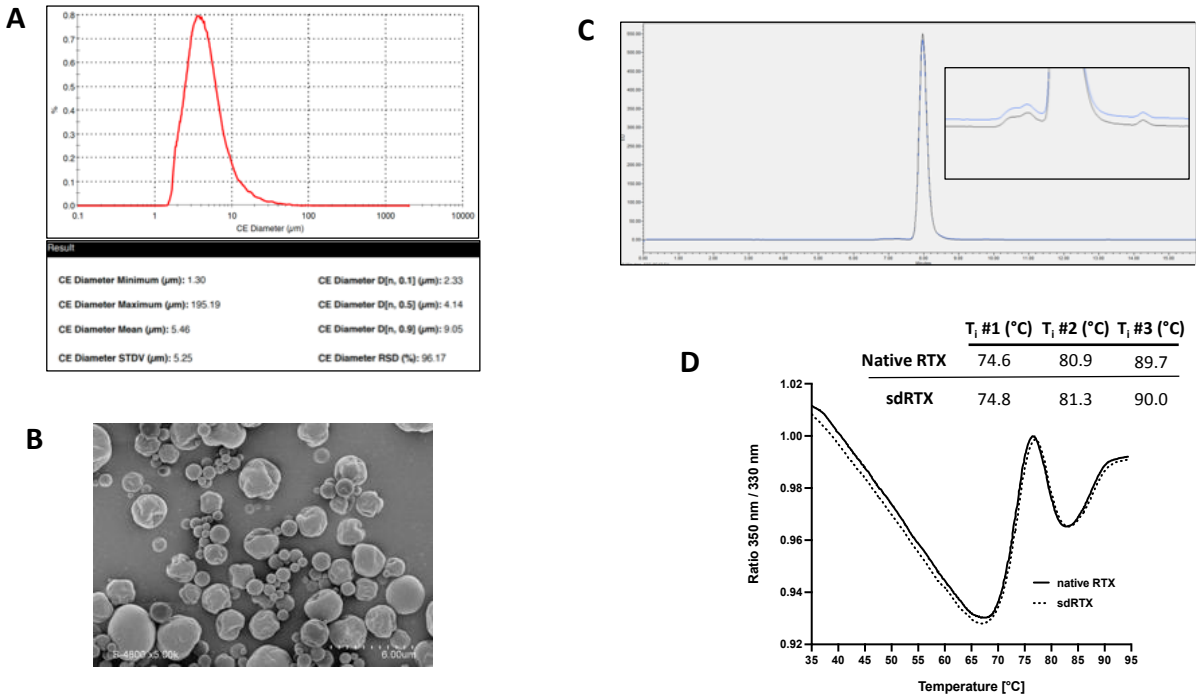

Fig. 1: Characterization of spray dried RTX*. (A) Particle size distribution analysis of the spray dried protein. (B) SEC-HPLC chromatograms of native RTX (black trace) and sdRTX (blue trace). The inset is a zoom on the elution peak baseline for a better visualization of HMW species. (C) SEM imaging of sdRTX powder. (D) Thermal analysis of native RTX (black trace) and sdRTX (dashed line). The ratio between the emitted fluorescence at 350 nm and 330 nm is represented in function of the temperature. Inflection temperatures (T_i) are indicated for both proteins.*

sdRTX was then dispersed into the V1 tripropionin-based polymeric vehicle presenting the TB1/DB1 polymer composition in a 1:1 ratio with a 20 % (w/w) total polymer content to yield the formulation named F1 (Table 1). The sd cake loading was 2.8 % (w/w) to achieve a 1.0 % (w/w) RTX loading in the final F1 formulation. The polymer concentration could have been increased to modify the sustained release properties of the formulation, but it was voluntarily kept low to make the formulation easily injectable through a 26 G needle for further *in vivo* evaluation. The *in vitro* dissolution profile of formulation F1 (TB1:DB1 polymer composition) was determined by making 100 mg depots (n=3) in the SEC-Tween release medium. We observed a S-shaped IVR profile consisting in an initial lag phase of 3 to 4 days followed by a

20-day steady release phase before reaching a plateau at around 70 % release of the injected cargo (Fig. 2A). Interestingly, the substitution of PBS to SEC-Tween as a release buffer accentuated the S-shaped release profile with a longer initial lag phase of around 10 days (Fig. 2A). For biocompatibility reasons, the PBS release medium was used for cell based and *in vivo* studies (see below). Independently of the release medium, the F1 formulation displayed promising *in vitro* sustained release properties and a good overall protein recovery as 10% to 15% of the initial protein cargo could be retrieved in the depots at the end of the release experiment. Of note, the onset of protein release coincided with the release of lactic acid in the release medium making the bridge between protein release and polymer degradation. However, an early-stage stability study showed that the HMW fraction increased significantly upon storage at 4°C for several weeks (Fig. 2B). In order to overcome this drawback, the composition of the sd protein cake was adjusted by adding trehalose, a disaccharide well-known to stabilize proteins during drying processes. Its presence substantially improved the protein stability within the BEPO® formulation by reducing the formation of HMW species (Fig. 2B).

With trehalose present in the sdRTX cake, the influence on the IVR profile of different parameters such as the diblock nature, the TB:DB ratio or the protein loading was investigated. A more hydrophobic diblock (DB2) considerably slowed down the release kinetics but conversely prevented a complete release of the protein cargo as the cumulative release profile plateaued at a 30 % release of the initially encapsulated antibody (Fig. 2C). Only 15 to 20 % of the drug cargo was retrieved at the end of the IVR study when protein was extracted and quantified from the remaining depots, which could be the signature of some irreversible protein binding to the polymer matrix that could be due to the hydrophobic nature of the diblock DB2 molecule. The change in the TB:DB ratio with a higher proportion of TB attenuated the S-shaped release profile and resulted in an almost linear release kinetics with a release rate of approximately 1 % of protein cargo per day, while unexpectedly the increase in protein loading did not accelerate the release. For this last formulation, loaded with 2 % of protein, 40 % of the initial protein cargo was retrieved in the depots at the end of the IVR study, leading to a similar

overall recovery as F1. Based on these results, for further investigations, we focused on the F1 formulation (1 % (w/w) RTX final loading in the V1 BEPO® vehicle.

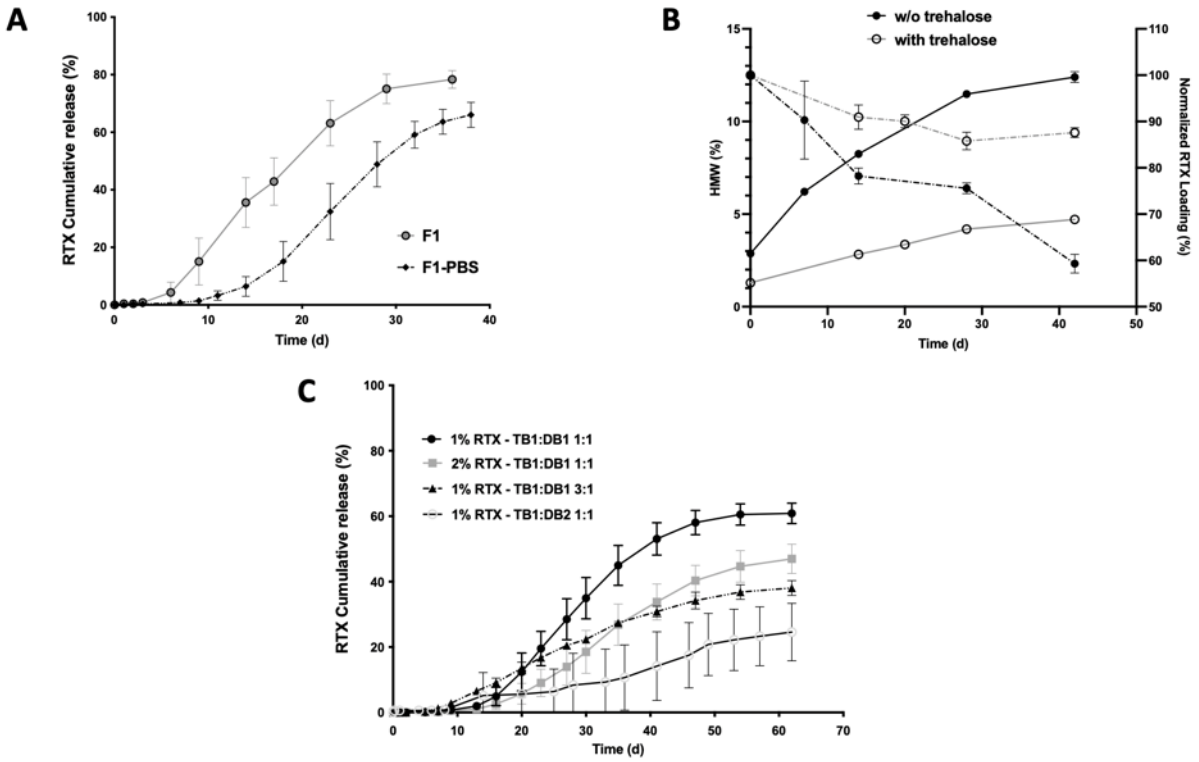

Fig. 2: In vitro dissolution profiles and stability of BEPO®:RTX formulations. *(A) In vitro release profiles of F1 formulation (TB1:DB1 polymer composition). (B) Impact of the presence of trehalose in the sd RTX cake on the stability of the F1 formulation stored at 4°C followed by SEC-HPLC (HMW fraction in plain lines, normalized protein loading in dashed lines). (C) Impact of variation of diblock, triblock type and ratio and drug loading in the formulation over in vitro release profile.*

Benefiting from the experience gathered while formulating RTX, we chose to formulate another mAb, daratumumab (DARA), an anti-CD38 antibody commercialized under the brand name Darzalex®. The commercial solution was buffer-exchanged for a trehalose containing solution and spray dried using the same conditions as those used for RTX. The particle size distribution of the sdDARA cake was similar to that of RTX and SEC-HPLC analysis demonstrated that the spray dried protein had a similar profile as the commercial one, especially in terms of HMW fraction (data not shown). sdDARA was then dispersed into the polymeric vehicle V1 to achieve

a 1 % (w/w) final protein loading. The resulting formulation presented an IVR profile similar to the one loaded with RTX but with an earlier onset of protein release (Suppl. Fig. S3). This supported our hypothesis that given our solid-state formulation approach, the identity of two proteins of similar chemical nature would have a minimal impact on a formulation with a selected polymer composition in terms of release characteristics.

5.2. Physico-chemical characterizations of formulated RTX

To monitor the potential generation of post-translational modifications (PTMs) during the formulation process, different physico-chemical analyses were carried out on the formulated protein. First, orthogonal LC methods were developed and RTX stability was assessed under two angles. First, the stability of the protein in the formulation was monitored during the subsequent storage of the formulation at 4°C during several weeks (daRTX samples, Suppl. Fig. S4). Also, the status of the released protein was evaluated during the course of an IVR study (ivRTX samples, Suppl. Fig. S4). In the latter, the concentration of the released protein was often too low to allow for a valid analysis. In consequence, as a surrogate, to avoid any protein concentration step that could be a bias, RTX was extracted from the solid polymer depots incubated at 37°C (depRTX samples, Suppl. Fig. S4) as a reflect of the released protein stability. RTX F1 formulation with trehalose was taken as the reference formulation for all these analyses.

The SEC-HPLC analysis of three independent studies showed that the fraction of HMW species increased steadily, almost linearly, upon storage at 4°C to reach around 5 % of HMW species after 10 weeks. Of note, the HMW fraction of the commercial protein is 0.6 % (Fig. 3A). SCX-HPLC analysis of the same samples showed a good stability of the charge variant distribution with a stable proportion of both acidic and basic variants (data not shown). RP-HPLC analysis after IdeS digestion highlighted the generation of a main impurity that was associated to the Fc moiety and presented a relative retention time of 0.95 compared to the Fc elution peak. Further mass spectrometry analysis showed that this impurity presented a mass adduct of +16 Da

corresponding most probably to the oxidation of a methionine residue. This impurity was noted oxMet Fc and its content was reported as the fraction of the Fc moiety elution peak area. Compared to the initial oxidized methionine content of 2.9 % for the native protein, methionine oxidation level increased upon formulation (4.4 % for the daRTX T0 samples) and the trend amplified during storage to reach almost 9 % after 10 weeks storage (Fig 3A). The stability pattern was more contrasted regarding the released protein. If the protein extracted from the depot (depRTX samples) presented a limited fraction of HMW species (4 % after four weeks incubation at 37°C in the polymeric matrix), it displayed a pronounced oxidation of methionine residues on the Fc moiety, up to 20% (Fig. 3B, left). The charge variant distribution changed also noticeably in the depot. SCX-HPLC revealed that native RTX presented acidic and basic variants that accounted respectively for 20 % and 6 % of the total peak area. The incubation within the depot led to a progressive disappearance of the basic variants and a concomitant increase of the proportion of acidic variants at the expense of the main peak relative area (Fig. 3B, right). To study more in-depth the stability profile of the formulated RTX, a full tryptic peptide mapping was undertaken. RTX has a well-known peptidic signature, which includes the following peptides: GLEWIGAIYPGNGDTSYNQK, ASGYTFTSYNMHWVK and FSGSGSGTSYSLTISR. For all tested samples, we obtained a proper sequence coverage, associated with a good confidence Mascot score and a reasonable quantity of detected peptides (Suppl. Fig. S5). Afterwards, the modification of three peptides of the heavy chain, each of them containing a methionine residue, was analyzed. The native RTX protein presented minimal methionine oxidation, the most noticeable one being observed on the residue Met35. Confirming previous observations made after IdeS digestion, LC-MS data showed that the formulation process enhanced the oxidation of methionine Met257. Increasing levels of oxMet257 were observed during formulation storage (daRTX samples), while highest levels were observed for the released protein (ivRTX samples). These same samples showed also an increased oxidation of the Met433 residue (Fig. 3C).

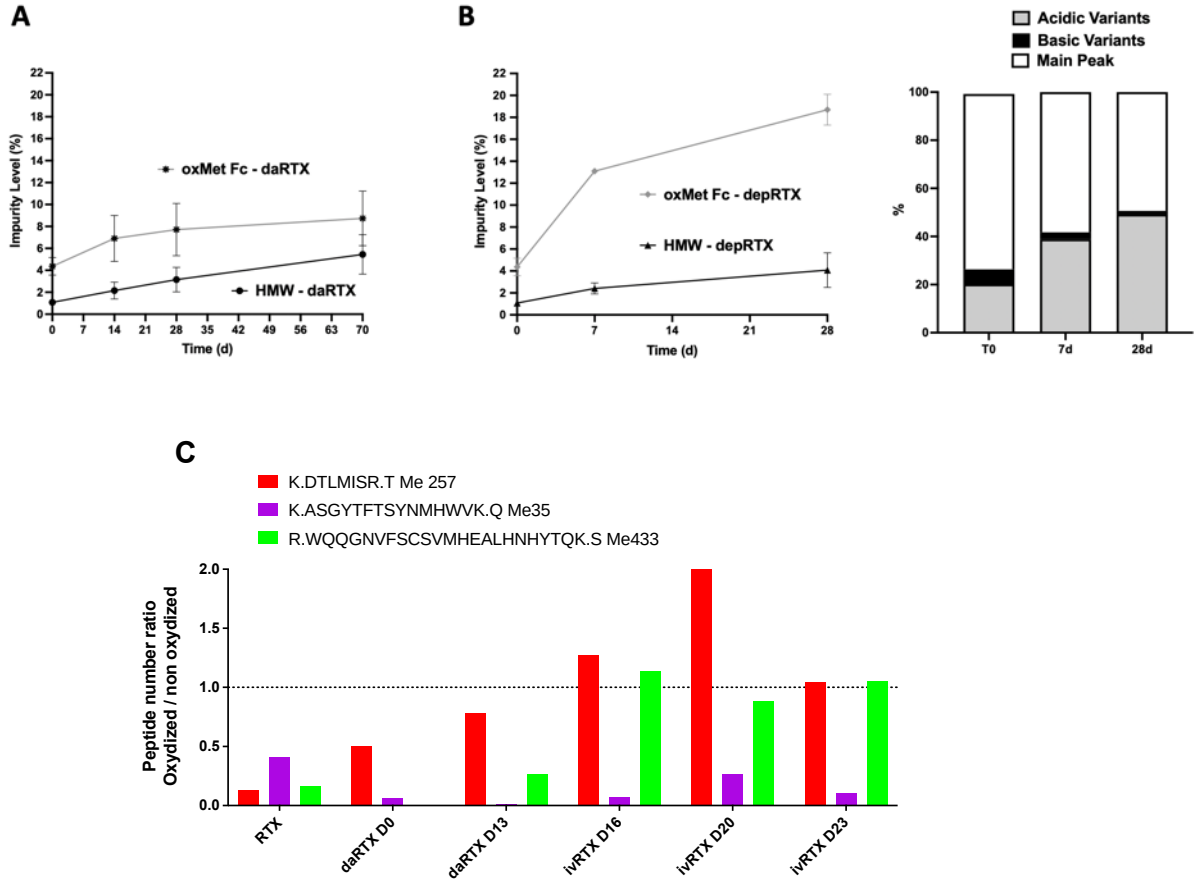

527

528 ***Fig. 3: Stability of formulated RTX***. *(A) Evolution of the HMW fraction and the Fc-related*
529 *oxidation impurities (oxMet Fc) during a 10-week storage at 4°C of a BEPO®:RTX formulation.*
530 *(B) Evaluation of the impurity pattern of depRTX samples for the protein extracted from the*
531 *polymer depots after 7 days and 28 days of incubation at 37°C through the three LC methods.*
532 *(C) For the same RTX samples, analysis by Q-tof Impact2 MS of the oxidation pattern of three*
533 *heavy chain peptides carrying out one methionine residue potentially sensitive to oxidation.*

534

535 The DTLMISR peptide carrying Met257 residue was under particular scrutiny, as several
536 studies have shown that this conserved methionine residue located in the Fc moiety of human
537 IgG1 is prone to oxidation, which could reduce the antibody binding affinity to the FcRn
538 receptor and hence imparts the antibody pharmacokinetics properties [24–26]. In an effort to
539 better evaluate the potential outcome of this PTM, the binding affinities of native and
540 formulated RTX to CD16a (FcγRIIIa), including the potential V158F polymorphism, CD16b
541 (FcγRIIIb) and FcRn receptors was measured *in vitro* by Surface Plasmon Resonance (SPR).
542 Table 2 shows that RTX extracted at different times from the formulation or polymer depots

showed similar binding affinities for those receptors as native protein, suggesting that the PTMs that had been evidenced on the Fc moiety had not reached a level that would alter RTX binding properties.

Table 2: Affinity of formulated RTX samples for CD16a, CD16b and FcRn receptors

Proteins	CD16a K_D pH 7.4 (M)	CD16a V158F K_D pH 7.4 (M)	CD16b K_D pH 7.4 (M)	FcRn K_D pH 6.0 (M)
Native RTX	2.74×10^{-7}	9.52×10^{-7}	15.40×10^{-7}	2.73×10^{-8}
daRTX T0	1.30×10^{-7}	2.69×10^{-7}	4.97×10^{-7}	2.47×10^{-8}
daRTX 5w 4°C	1.13×10^{-7}	1.99×10^{-7}	5.72×10^{-7}	2.63×10^{-8}
depRTX 7d	1.00×10^{-7}	1.33×10^{-7}	2.96×10^{-7}	2.67×10^{-8}
depRTX 13d	0.92×10^{-7}	1.06×10^{-7}	2.19×10^{-7}	2.64×10^{-8}

5.3. Biological activity of formulated mAbs

We then investigated the protein biological activity through different approaches. First, the capacity of sdRTX to generate antibody-dependent cell cytotoxicity (ADCC), a process that requires recognition of the Fc moiety by the CD16 receptor expressed by NK cells and the recognition of CD20 on the plasma membrane of target cells (*i.e.* Raji cells) by the Fab moiety, was analyzed. It was firstly observed that sdRTX bound Raji cells like RTX and induced ADCC with a similar efficiency than RTX (Suppl. Fig. S6). This showed that the spray drying process did not alter the protein functionality.

Next, we studied the CD20 binding activity of various formulated RTX samples by flow cytometry. The selected samples obtained from formulated, depot-extracted or in vitro released RTX displayed similar binding activity than the native RTX (Fig. 4A). Moreover, the same observations were essayed for CD16 binding using the Jurkat-NFAT reporter assay (Suppl. Fig. S7). Altogether, these results suggested that Fab and Fc moieties of RTX were both still functional during the formulation process.

To further investigate antibody-based effector functions, the capability of RTX to elicit ADCC against two CD20+ vcell lines, Raji and Daudi, was evaluated. RTX or NK cells alone induced

cell death, while their concomitant addition provoked a synergistic effect (Fig. 4B and C and Suppl. Fig. S8). Again, formulated RTX (daRTX, ivRTX and depRTX) samples induced similar ADCC than the native RTX (Fig. 4B and 4C). In summary, taken together, these results demonstrate that a BEPO® derived depot released a fully functional RTX protein. Additionally, the biological activity of RTX extracted from an ISFD formulation after several weeks of storage at 4°C was clearly established.

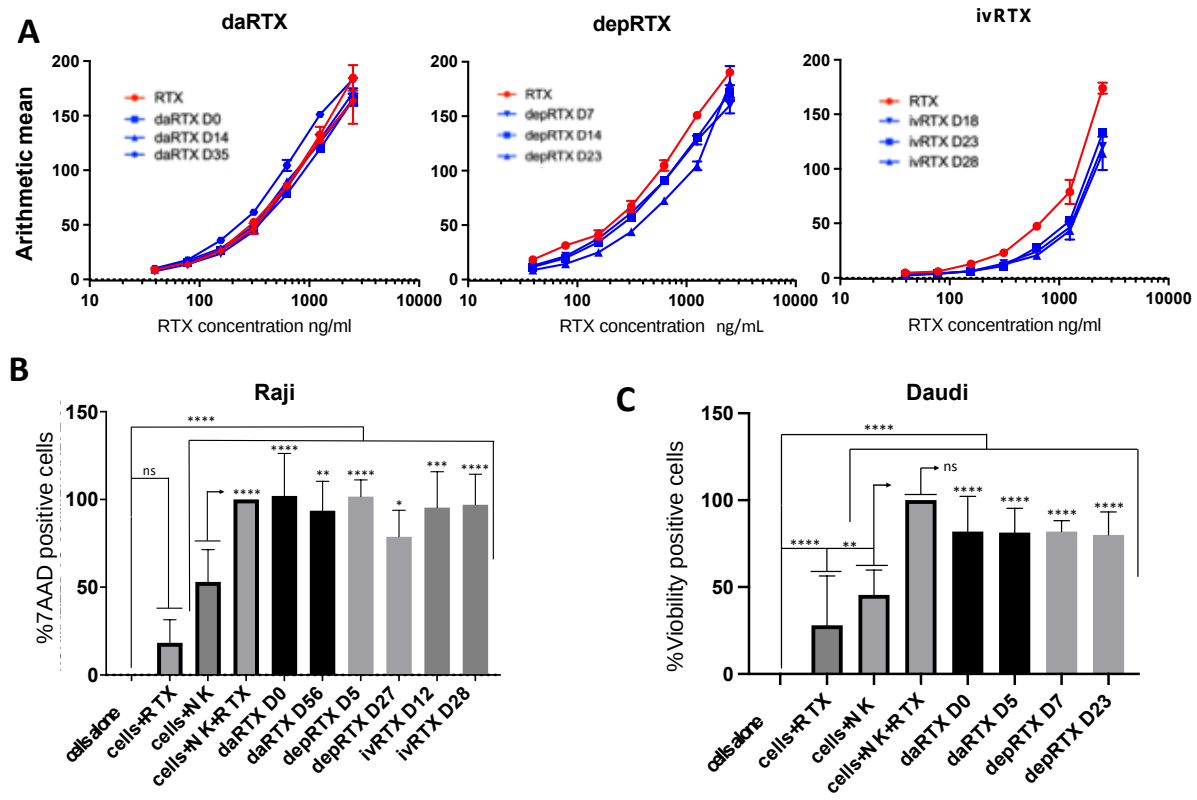

Fig. 4: Functionality of formulated RTX. *All RTX samples were obtained from the same BEPO®:RTX formulation (F1 with trehalose) and were either extracted from the formulation after storage at 4°C (daRTX samples) or obtained during the release study through the evaluation of the released protein (ivRTX) or the extraction of the protein from the solid polymer depot (depRTX) at different time points. (A) Binding of RTX to CD20 on Raji cells, as expressed as the arithmetic mean fluorescence intensity (MFI). B-C) ADCC assay with different RTX samples (10 µg/ml), in presence of NK cells (E:T, 3:1) carried out overnight on Raji cells using 7AAD staining (B) or after 8 hours on Daudi cells using viobility™ staining (C). Basal*

*cell death was normalized to 0% and commercial RTX+NK cells to 100%. Sample activity was presented as % of native RTX activity. Graphs show mean+/- SD of a minimum of 2 experiments performed in triplicate. Samples were compared by 2-ANOVA test, n = 21, * p < 0.05, ** p < 0.01 *** p < 0.001; **** p < 0.0001.*

Functionality of formulated DARA was also evaluated using a pseudo-ADCC assay. As CD38 is present at the surface of NK cells, these cells served both as target and effector cells. In consequence, the incubation of DARA with NK cells should lead to their rapid death if both antibody moieties retain their functionality. Indeed, DARA significantly raised NK cell death by an average of 26% and da, dep and sdDARA samples from formulated DARA exhibited similar effects (Fig. 5).

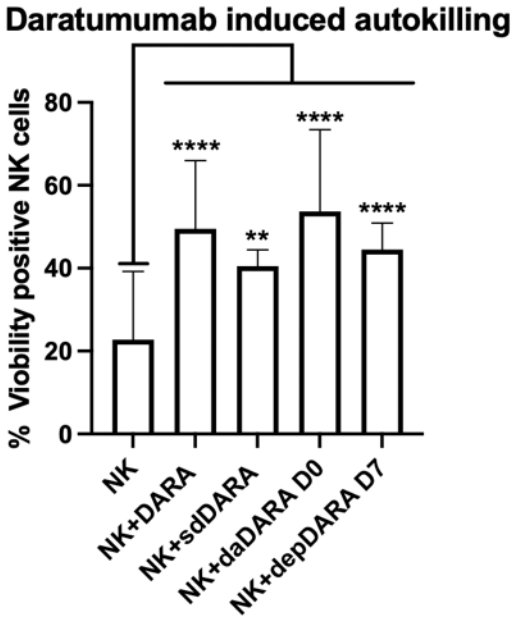

Fig. 5: Functionality of formulated DARA evaluated through NK cells autokilling.

DARA samples were obtained and extracted from the BEPO®:DARA formulation presenting the TB1:DB1 polymer composition. sdDARA was the spray dried protein solubilized in PBS, daDARA D0 was the protein extracted from the formulation just after reconstitution while depDARA D7 was obtained after the extraction of the protein from the solid polymer depot 7 days after depot formation.

The *in vivo* biological activity of the RTX F1 formulation was further assessed in a subcutaneous xenograft model of the human CD20+ lymphoma cell line BCL-P2 in NSG mice. A rapid tumor growth was observed and overall survival was shorter than 25 days (Fig. 6A). While non-significant improvements were made by regular NK cells injection, intravenous treatment with saline RTX largely decreased tumor growth and increased mice survival independently of NK cell engraftment. Subcutaneous injection of F1 formulation was as effective as saline RTX and, in fact, tumor initial growth was delayed and mice survived longer, demonstrating the full *in vivo* functionality of the formulated RTX (Fig. 6B).

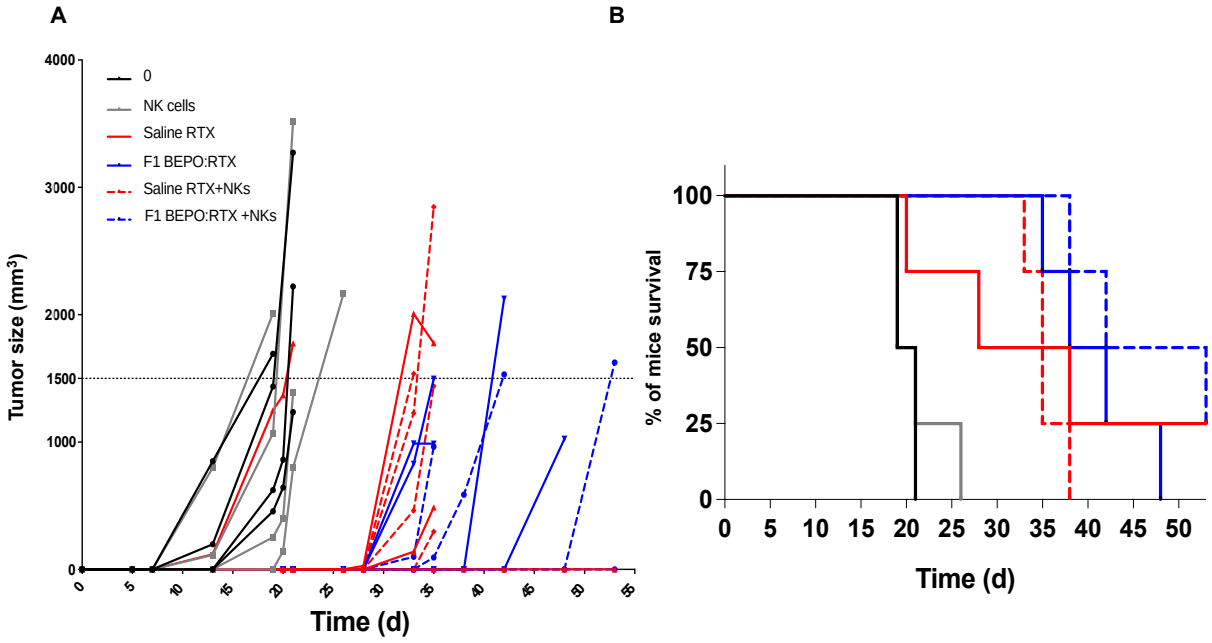

Fig. 6: Evaluation of RTX functionality in a model of B cell lymphoma cell xenograft into NSG mice. *5 millions of BCL-P2 lymphoma B cells were grafted into NSG mice. (A)Evolution of the tumor size after tumor cell engraftment. (B) Survival curves representing the percentage of animals with tumor size under 1500 mm^3 in function of days after tumor cell inoculation.*

5.4. Intra-articular delivery

Because of the generation of a drug reservoir upon injection, *in situ* forming depot technologies are especially relevant to locally increase mAb concentration in, or close to, the target tissue. In this study, mAb ISFD formulations were tested using the intra-articular (IA) route of

administration. First, biocompatibility was evaluated over 28 days after IA injection of the V1 polymeric vehicle with or without RTX. In contrast to the RTX saline solution, both vehicle and RTX formulation induced an initial inflammatory reaction that partly resolved over time (Fig. 7A, left). The pattern was typical of a foreign body reaction. The higher inflammatory reaction noticed for the formulation could be due to the formulation of a non-murine protein as RTX is a chimeric antibody that presents murine variable and human constant regions. Indeed, anti-drug antibodies (ADAs), *i.e.* anti-RTX antibodies, were detected in the serum of treated animals, which could be related with the exacerbated inflammation (Fig. 7B).

This hypothesis was supported by the fact that IA injection of a fully murine protein (mRTX) formulated with BEPO® led to lower inflammation levels compared to those generated with the chimeric antibody (Fig. 7A, right). Moreover, formulation of a rat IgG2A isotype generated a similar inflammation than the humanized RTX (Fig. 7A, right). Still, inflammation was going down at day 28. Of note, biocompatibility of the injected material was confirmed by the fact that no cartilage or subchondral bone damage could be detected after staining with safranin O Fast green (Fig. 7C).

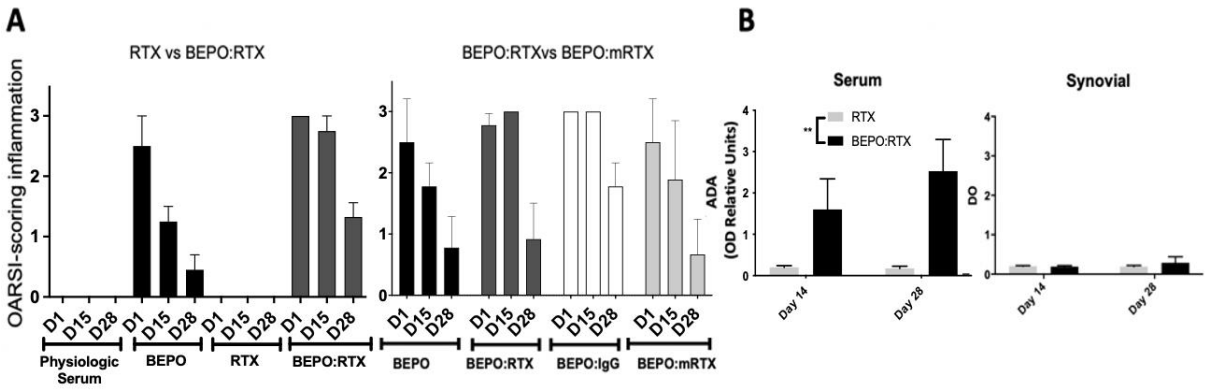

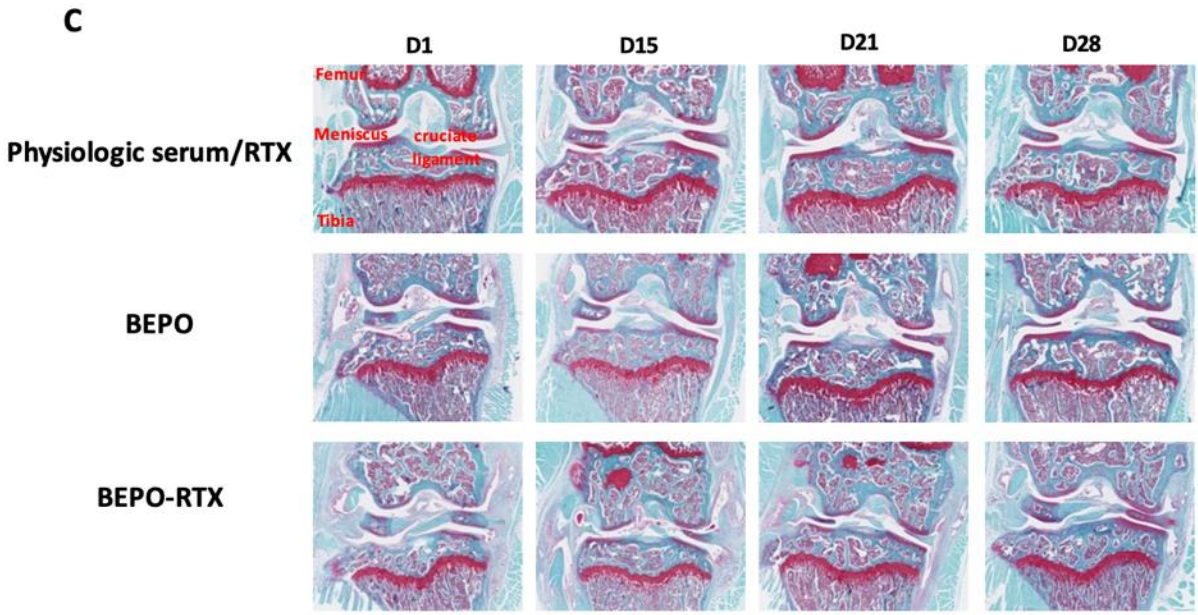

Fig. 7: Biocompatibility of BEPO® vehicles and formulations after IA delivery in mice. *(A) 3 C57BL/6J mice/group/timepoint were injected with saline RTX or ISFD formulations of* RTX, *rat IgG2b or mRTX in the intra-articular space of their right knee to achieve a 25µg protein dose. The OARSI inflammation score ranged from 0 to 3 was analyzed at different times after treatment. (B) Anti-drug antibodies profile for RTX (grey) and BEPO®:RTX (black) in serum and synovial fluid at 14 and 28 days in mice from (A). (C) Representative knee sections from mice from (A) at day 1, 15, 21 and 28.*

Next, we investigated the pharmacokinetics (PK) properties of the RTX F1 formulation. RTX was administered IA either as a saline solution or formulated with BEPO® (25 µg/2.5 µL). The resulting RTX concentrations in serum and in synovial fluid of the injected knee were measured over four weeks. In the saline group, the protein was mostly found in the systemic circulation as the C_{max} value normalized by the dose (7.3 (µg/mL)/(mg/kg)) was similar to the one that was obtained after subcutaneous administration of a RTX saline solution (Fig. 8A). RTX concentration in serum decreased following a 10-14 days half-life. As expected, the synovial fluid concentration was a fraction (around 10-fold lower) of that of serum. In contrast, IA injection of the F1 formulation allowed high synovial fluid concentrations sustained for four weeks with low systemic release. No RTX was retrieved in serum from 14 days post-inoculation

(Fig. 8A). The ratio between the synovial and serum concentrations at day 14 illustrated the differences as it was 0.13 for the saline group and 101 for the BEPO® group.

As RTX triggered the generation of anti-RTX antibodies, we repeated the experiment using murine RTX (mRTX). This latter formulation allowed sustained high synovial mRTX concentrations for 14 days, which was less pronounced than for the RTX formulation (Fig 8B). Still, the mRTX synovial to serum concentration ratio was greater than 1 at day 14. The faster clearing of mRTX from synovial fluid could be due to its binding to Fc receptors present at the surface of immune cells, which could accelerate synovial clearance.

To avoid generation of ADA and challenge our local delivery approach with a new mAb, we administered IA the DARA protein into the right knee of immune suppressed NSG mice, which lack B cells and hence antibody production. The clearance of human IgG1 is considerably accelerated in these mice [27], a feature that we retrieved in our study as DARA was not quantifiable anymore in the serum of the animals 10 days after IA injection of saline DARA (Fig. 8C). DARA also had disappeared from synovial fluid at this time. We then dispersed sdDARA into V1 polymeric vehicle at 1 % (w/w) and 25 µg of the resulting formulation was IA injected. At day 10, DARA could not be detected in serum. However, it was still present in synovial fluid 30 days after administration (Fig. 8C). In summary, these data demonstrate that formulating mAbs with BEPO® allowed high local protein concentrations for several weeks.

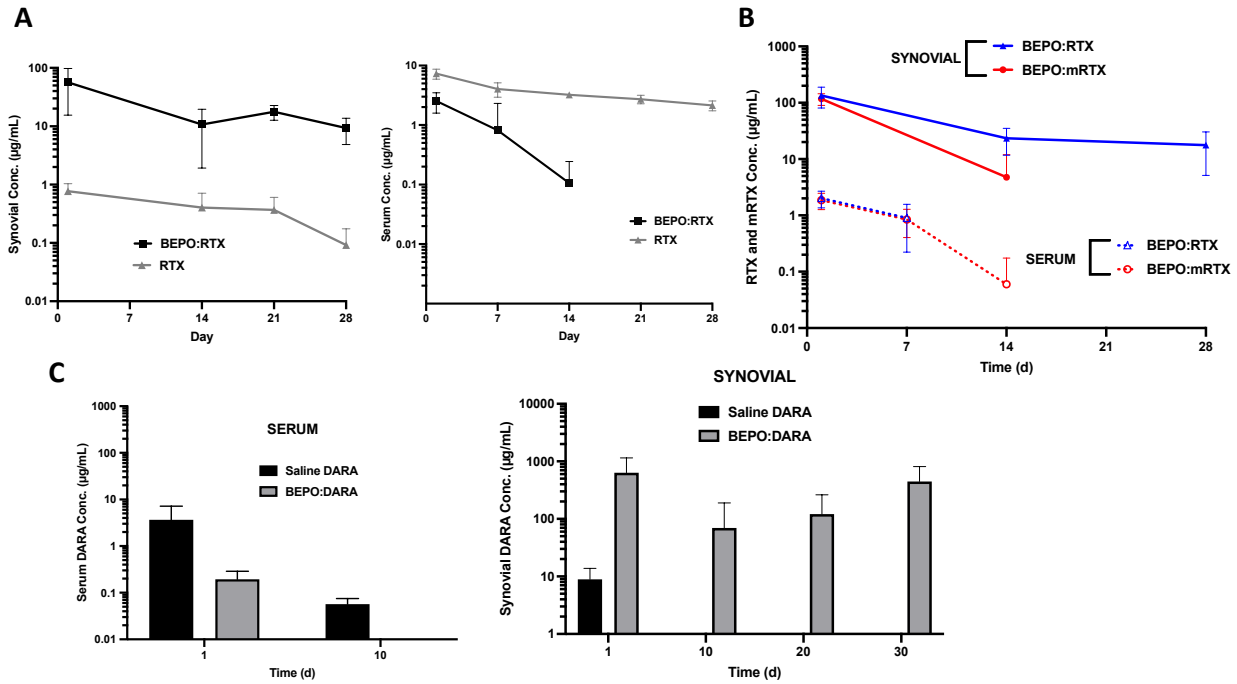

Fig. 8: Pharmacokinetics studies of BEPO:mAb formulations after intra-articular administration. *(A) 3 C57BL/6J mice/group/timepoint were injected with saline RTX or BEPO®:RTX formulation in the intra-articular space of their right knee to achieve a 25µg protein dose. RTX was quantified using a specific ELISA assay in both serum and knee synovial fluid at different times after treatment. (B) PK profiles of two BEPO® formulations incorporating either RTX or the fully murine mRTX protein. (C) 4 NSG mice/group were injected with saline DARA or BEPO®:DARA formulation in the intra-articular space of their right knee to achieve a 16 µg protein dose. DARA was quantified by ELISA in both serum and knee synovial fluid at different times after treatment.*

6. DISCUSSION

The design of long-acting injectable protein formulations through the use of bioresorbable polymers has always represented a daunting task especially regarding the preservation of the protein integrity and functionality. In fact, there are currently no commercialized products of a therapeutic protein formulated with polyesters such as PLGA or PLA [28,29]. In order to minimize the generation of impurities due to interactions between protein and polymer, we opted for a strategy, in which the protein would stay in its solid state during the entire

formulation process. This approach had been used successfully to formulate a Fab fragment with PLGA and, more recently, we managed to formulate a 55 kDa bispecific antibody with PEG-PLA copolymers [17,30]. It requires the production of a protein powder, which in our case was obtained via a spray drying process. Along lyophilization, spray drying has become a method of choice to produce protein powders[31,32]. We confirmed that two clinically relevant mAbs, namely RTX and DARA, were not altered by the spray drying process and retained their functionality. Only a very slight increase of the HMW fraction was observed, an increase that amplified during the formulation process. However, the generation of aggregates in the formulation could be largely circumvented with the introduction of trehalose, a well-known protein stabilizer during drying processes [33,34]. HMW fraction is a critical quality attribute of therapeutic proteins as the presence of aggregates is often linked to immunogenicity issues. A 5% limit is usually set as a specification for therapeutic mAb formulations in the pharmaceutical industry and the presence of trehalose allowed to stay below this level even after several weeks of storage at 4°C. Still, as most of antibody preparations present HMW fractions below 2% [33,34], it should guide us to try to further improve the stability profile of the formulated proteins.

Because local delivery requires usually the use of relatively low doses of the therapeutic molecule, a low protein loading of 1 % (w/w) was chosen for the BEPO®:mAb formulation. Also, polymer concentration was chosen to yield a formulation viscosity compatible with an administration through a 26 G needle for further *in vivo* evaluations. Different IVR profiles were generated, and we showed that different parameters in the formulation such as the polymer composition could change the release kinetics. While the formulated protein showed a good stability profile in the formulation stored at 4°C for several weeks, the protein released from the polymer depots showed different PTMs revealed by a change in the charge variant distribution as well as an increase of methionine oxidation on the Fc moiety. However, SPR showed that these modifications did not alter the RTX binding affinities to several Fc receptors. Moreover, *in vitro* cell-based assays showed that the functionality of formulated mAbs was

similar to those of the commercial products and full biological activity of formulated RTX was demonstrated in a xenografted mice model. Thus, it can be concluded that our BEPO®:mAb formulations released a protein with similar functional properties to the clinical ones.

Our second goal was to evaluate the pertinence of using such formulations for local delivery. IA delivery is of particular interest as there are considerable unmet medical needs for the treatment of rheumatic diseases and particularly of rheumatoid arthritis where 30% of patients are resistant to biotherapies and osteoarthritis [35]. This delivery route associated with a drug delivery system would undoubtedly improve the efficacy of treatments, as past and recent clinical trial failures with systemic delivery of therapeutic proteins could be attributed to a lack of synovial fluid exposure [36–38]. Here, we showed that the IA injection of BEPO®:mAb formulations allowed to sustain high synovial fluid concentration of the antibody for several weeks in the knee of mice in contrast to saline compositions. The formulation induced inflammation locally, which could be related to the high quantity of foreign material injected relative to the size of the mouse joint. In agreement with this hypothesis, the inflammatory reaction disappeared overtime, probably in relation with the progressive polymer resorption. Importantly, no cartilage or subchondral bone damage was detected. It would be interesting in the future to better evaluate the inflammatory process in an animal species that presents a larger synovial fluid volume. Another important observation was the higher inflammation levels that were observed for BEPO®:mAbs formulations compared to the corresponding BEPO® vehicles or protein saline solutions. This phenomenon could be related to the generation of ADAs produced in BEPO®:RTX administered animals. The mouse immune system should recognize RTX as a foreign antigen and reacts generating ADAs. B-cells can be activated to plasma cells by antigens possessing repetitive epitopes which cross-link antigen-specific BCR, breaking down B-cell tolerance [39,40]. The faculty of well-ordered structures to induce more potent immune responses compared with monomeric proteins has been known for decades [41] and is at the basis for new vaccine generation [42-45]. A breakdown in tolerance following the formation of repetitive epitopes probably induces ADA [39]. The release process from the

polymeric depot, that is associated with the progressive solubilization of the embedded spray dried protein cake should promote very high local RTX concentrations that could induce the formation of subvisible particles or repetitive-like epitopes that can greatly enhance immunogenicity. In addition, the presence of an inflammatory context due to the presence of a foreign body, i.e. BEPO, could also play a role in the generation of ADA. Therefore, the potential immunogenicity of a BEPO:RTX formulation will have to be studied more in-depth in the future as high ADA titers could hamper the clinical development of such a product especially for a chronic administration. However, it is interesting to note that very concentrated epitopes, protein aggregation, repeat dosage and prolonged exposure may either break or lead to tolerance [40,46], which suggests that the product final immunogenicity could be uncovered only after its clinical use.

Finally, BEPO®:DARA formulation confirmed the results that we had generated with the RTX protein in terms of preservation of protein integrity and functionality and the PK study in NSG mice highlighted once again the pharmacokinetics promises held by such formulations. Taken together, the results shown in the present paper demonstrate that intra-articular delivery of BEPO®:mAb formulations could enable future treatments by increasing considerably the synovial fluid:plasma concentration ratio, which could improve treatment efficacy while lower potential side effects.

7. CONCLUSION

The BEPO® delivery platform offers a simple and effective tool to design long-acting injectable therapeutic protein formulations, preserving their functionality and minimizing the generation of PTMs. Moreover, after intra-articular administration, BEPO®:mAb formulations demonstrated superior pharmacokinetics properties compared to IA saline bolus of the same protein. This could improve the efficacy of future treatments in a therapeutic area where there are still high unmet medical needs. It will be important in the future to confirm and expand our data in larger animal species and exploit the BEPO® features for other modes of local delivery.

Acknowledgements

We acknowledge the imaging facility MRI, the Montpellier platform of EcellFrance, a national infrastructure supported by the PIA and the French National Research Agency (ANR-11-INBS-0005). We thank Martine Pugnière (IRCM, Montpellier) for the Biacore experiments. This work also benefited from umbilical cord blood units (UCBs) and the expertise of Prof. John De Vos, in charge of the Biological Resource Center Collection of the University Hospital of Montpellier –http://www.chu-montpellier.fr/

Author Contributions Statement

A.F., W.L., S.G., D.N., P.LP. and M.V. designed experiments. A.F., K.T. and S.G. performed experiments and analyzed results. A.F., M.V. and S.G. wrote the main manuscript text. All authors reviewed and approved the manuscript.

Ethical statement

S.G. and A.LN. are MedinCell employees. S.G., W.L. and A.LN. are shareholders of MedinCell. Other authors declare no competing financial interests.

Funding

This work was supported by institutional funding from INSERM and University of Montpellier, by funding from the Region Occitanie (GRAINE /Project LiCAtherAO), and by the PRT-K program 2018 (MV 2018-021) and the LabEx MAbImprove: ANR-10-LABX-53 (MV/PP).

Data Availability

The authors confirm that the data supporting the findings of this study are available within the article [and/or] its supplementary materials.

References

[1] D.W. Grainger, V Controlled-release and local delivery of therapeutic antibodies, Expert Opinion on Biological Therapy. 4 (2004) 1029–1044. https://doi.org/10/cmhfz4.

[2] R.G.A. Jones, A. Martino, Targeted localized use of therapeutic antibodies: a review of non-systemic, topical and oral applications, Crit Rev Biotechnol. 36 (2016) 506–520. https://doi.org/10/gfw6cz.

[3] R.E. Kontermann, Strategies for extended serum half-life of protein therapeutics, Curr Opin Biotechnol. 22 (2011) 868–876. https://doi.org/10/fwv5ht.

[4] I. Elron-Gross, Y. Glucksam, R. Margalit, Liposomal dexamethasone–diclofenac combinations for local osteoarthritis treatment, International Journal of Pharmaceutics. 376 (2009) 84–91. https://doi.org/10/bpcxxq.

[5] M. Morgen, D. Tung, B. Boras, W. Miller, A.-M. Malfait, M. Tortorella, Nanoparticles for Improved Local Retention after Intra-Articular Injection into the Knee Joint, Pharmaceutical Research. 30 (2013) 257–268. https://doi.org/10/f4h9pt.

[6] R.G.A. Jones, A. Martino, Targeted localized use of therapeutic antibodies: a review of non-systemic, topical and oral applications, Critical Reviews in Biotechnology. (2015) 1–15. https://doi.org/10/gfw6cz.

[7] D.W. Grainger, V Controlled-release and local delivery of therapeutic antibodies, Expert Opinion on Biological Therapy. 4 (2004) 1029–1044. https://doi.org/10.1517/14712598.4.7.1029.

[8] F. Carubbi, L. Zugaro, P. Cipriani, A. Conchiglia, L. Gregori, C. Danniballe, M. Letizia Pistoia, V. Liakouli, P. Ruscitti, F. Ciccia, G. Triolo, C. Masciocchi, R. Giacomelli, Safety and efficacy of intra-articular anti-tumor necrosis factor α agents compared to corticosteroids in a treat-to-target strategy in patients with inflammatory arthritis and monoarthritis flare, Int J Immunopathol Pharmacol. 29 (2016) 252–266. https://doi.org/10/gf8pzr.

[9] U. Angkawinitwong, S. Awwad, P.T. Khaw, S. Brocchini, G.R. Williams, Electrospun formulations of bevacizumab for sustained release in the eye, Acta Biomater. 64 (2017) 126–136. https://doi.org/10/gfv9r5.

[10] M.-C. Robert, M. Frenette, C. Zhou, Y. Yan, J. Chodosh, F.A. Jakobiec, A.M. Stagner, D. Vavvas, C.H. Dohlman, E.I. Paschalis, A Drug Delivery System for Administration of Anti–TNF-α Antibody, Transl Vis Sci Technol. 5 (2016). https://doi.org/10/ggzn4n.

[11] S. Fogli, M. Del Re, E. Rofi, C. Posarelli, M. Figus, R. Danesi, Clinical pharmacology of intravitreal anti-VEGF drugs, Eye (Lond). 32 (2018) 1010–1020. https://doi.org/10/gdrkks.

[12] A. Usui-Ouchi, M. Friedlander, Anti-VEGF therapy: higher potency and long-lasting antagonism are not necessarily better, J Clin Invest. 129 (2019) 3032–3034. https://doi.org/10/gjp7kq.

[13] A. Marabelle, L. Tselikas, T. de Baere, R. Houot, Intratumoral immunotherapy: using the tumor as the remedy, Ann Oncol. 28 (2017) xii33–xii43. https://doi.org/10/gc2vnp.

[14] M. Tabrizi, G.G. Bornstein, H. Suria, Biodistribution Mechanisms of Therapeutic Monoclonal Antibodies in Health and Disease, (n.d.) 11. https://doi.org/10/b6ptk5.

[15] C.H. Evans, V.B. Kraus, L.A. Setton, 2013-11-5 Progress in intra-articular therapy, Nature Reviews Rheumatology. 10 (2013) 11–22. https://doi.org/10/gfw8ww.

[16] C. Roberge, J.-M. Cros, J. Serindoux, M.-E. Cagnon, R. Samuel, T. Vrlinic, P. Berto, A. Rech, J. Richard, A. Lopez-Noriega, BEPO®: Bioresorbable diblock mPEG-PDLLA and triblock PDLLA-PEG-PDLLA based in situ forming depots with flexible drug delivery kinetics modulation, Journal of Controlled Release. 319 (2020) 416–427. https://doi.org/10/gjkm5n.

[17] W. Leconet, H. Liu, M. Guo, S. Le Lamer-Déchamps, C. Molinier, S. Kim, T. Vrlinic, M. Oster, F. Liu, V. Navarro, J.S. Batra, A.L. Noriega, S. Grizot, N.H. Bander, Anti-PSMA/CD3 Bispecific Antibody Delivery and Antitumor Activity Using a Polymeric Depot

Formulation, Molecular Cancer Therapeutics. 17 (2018) 1927–1940. https://doi.org/10/gd9344.
[18] B. Philip, E. Kokalaki, L. Mekkaoui, S. Thomas, K. Straathof, B. Flutter, V. Marin, T. Marafioti, R. Chakraverty, D. Linch, S.A. Quezada, K.S. Peggs, M. Pule, A highly compact epitope-based marker/suicide gene for easier and safer T-cell therapy, Blood. 124 (2014) 1277–1287. https://doi.org/10/f6jxsr.
[19] N. Allende-Vega, E. Krzywinska, S. Orecchioni, N. Lopez-Royuela, F. Reggiani, G. Talarico, J.-F. Rossi, R. Rossignol, Y. Hicheri, G. Cartron, The presence of wild type p53 in hematological cancers improves the efficacy of combinational therapy targeting metabolism, Oncotarget. 6 (2015) 19228. https://doi.org/10/f727hd.
[20] S. Belkahla, A.U. Haq Khan, D. Gitenay, C. Alexia, C. Gondeau, D.-N. Vo, S. Orecchioni, G. Talarico, F. Bertolini, G. Cartron, J. Hernandez, M. Daujat-Chavanieu, N. Allende-Vega, M.V. Gonzalez, Changes in metabolism affect expression of ABC transporters through ERK5 and depending on p53 status, Oncotarget. 9 (2017) 1114–1129. https://doi.org/10/gjqv6z.
[21] D. Sanchez-Martinez, N. Allende-Vega, S. Orecchioni, G. Talarico, A. Cornillon, D.-N. Vo, C. Rene, Z.-Y. Lu, E. Krzywinska, A. Anel, E.M. Galvez, J. Pardo, B. Robert, P. Martineau, Y. Hicheri, F. Bertolini, G. Cartron, M. Villalba, Expansion of allogeneic NK cells with efficient antibody-dependent cell cytotoxicity against multiple tumors, Theranostics. 8 (2018) 3856–3869. https://doi.org/10/gd2c2x.
[22] D. Sánchez-Martínez, P.M. Lanuza, N. Gómez, A. Muntasell, E. Cisneros, M. Moraru, G. Azaceta, A. Anel, L. Martínez-Lostao, M. Villalba, L. Palomera, C. Vilches, J.A. García Marco, J. Pardo, Activated Allogeneic NK Cells Preferentially Kill Poor Prognosis B-Cell Chronic Lymphocytic Leukemia Cells, Frontiers in Immunology. 7 (2016). https://doi.org/10/ggzn4w.
[23] E. Krzywinska, A. Cornillon, N. Allende-Vega, D.-N. Vo, C. Rene, Z.-Y. Lu, C. Pasero, D. Olive, N. Fegueux, P. Ceballos, Y. Hicheri, M. Sobecki, J.-F. Rossi, G. Cartron, M. Villalba, 2016 04 CD45 Isoform Profile Identifies Natural Killer (NK) Subsets with Differential Activity, PLOS ONE. 11 (2016) e0150434. https://doi.org/10/ggzn4p.
[24] J. Mo, Q. Yan, C.K. So, T. Soden, M.J. Lewis, P. Hu, Understanding the Impact of Methionine Oxidation on the Biological Functions of IgG1 Antibodies Using Hydrogen/Deuterium Exchange Mass Spectrometry, Anal. Chem. 88 (2016) 9495–9502. https://doi.org/10/f86xhc.
[25] Selective Oxidation of Methionine and Tryptophan Residues in a Therapeutic IgG1 Molecule - Folzer - 2015 - Journal of Pharmaceutical Sciences - Wiley Online Library, (n.d.). https://onlinelibrary.wiley.com/doi/full/10.1002/jps.24509 (accessed April 5, 2021).
[26] A. Bertolotti-Ciarlet, W. Wang, R. Lownes, P. Pristatsky, Y. Fang, T. McKelvey, Y. Li, Y. Li, J. Drummond, T. Prueksaritanont, J. Vlasak, Impact of methionine oxidation on the binding of human IgG1 to Fc Rn and Fc gamma receptors, Mol Immunol. 46 (2009) 1878–1882. https://doi.org/10/cwm6wg.
[27] R.J. Oldham, C.I. Mockridge, S. James, P.J. Duriez, H.T.C. Chan, K.L. Cox, V.A. Pitic, M.J. Glennie, M.S. Cragg, FcγRII (CD32) modulates antibody clearance in NOD SCID mice leading to impaired antibody-mediated tumor cell deletion, J Immunother Cancer. 8 (2020) e000619. https://doi.org/10/gjnfk6.
[28] S.P. Schwendeman, R.B. Shah, B.A. Bailey, A.S. Schwendeman, Injectable controlled release depots for large molecules, Journal of Controlled Release. 190 (2014) 240–253. https://doi.org/10/f6sjp9.
[29] R. Vaishya, V. Khurana, S. Patel, A.K. Mitra, Long-term delivery of protein therapeutics, Expert Opin Drug Deliv. 12 (2015) 415–440. https://doi.org/10/gfv9sx.
[30] D.P. Chang, V.K. Garripelli, J. Rea, R. Kelley, K. Rajagopal, 2015 10 Investigation of Fragment Antibody Stability and Its Release Mechanism from Poly(Lactide-co-Glycolide)-Triacetin Depots for Sustained-Release Applications, Journal of Pharmaceutical Sciences. 104 (2015) 3404–3417. https://doi.org/10/f7q372.

[31] B. Gikanga, R. Turok, A. Hui, M. Bowen, O.B. Stauch, Y.-F. Maa, Manufacturing of High-Concentration Monoclonal Antibody Formulations via Spray Drying—the Road to Manufacturing Scale, PDA Journal of Pharmaceutical Science and Technology. 69 (2015) 59–73. https://doi.org/10/ggr34b.
[32] M. Batens, J. Massant, B. Teodorescu, G. Van den Mooter, Formulating monoclonal antibodies as powders for reconstitution at high concentration using spray drying: Models and pitfalls, European Journal of Pharmaceutics and Biopharmaceutics. 127 (2018) 407–422. https://doi.org/10/gdpf8c.
[33] N.K. Jain, I. Roy, Effect of trehalose on protein structure, Protein Sci. 18 (2009) 24–36. https://doi.org/10/c4r7td.
[34] K. Rajagopal, D. Chang, P. Nayak, S. Izadi, T. Patapoff, J. Zhang, R. Kelley, A. Sreedhara, Trehalose Limits Fragment Antibody Aggregation and Influences Charge Variant Formation in Spray-Dried Formulations at Elevated Temperatures, Mol. Pharmaceutics. 16 (2019) 349–358. https://doi.org/10/gjq5g7.
[35] A. Latourte, M. Kloppenburg, P. Richette, Emerging pharmaceutical therapies for osteoarthritis, Nat Rev Rheumatol. 16 (2020) 673–688. https://doi.org/10/gjq5gg.
[36] X. Chevalier, P. Goupille, A.D. Beaulieu, F.X. Burch, W.G. Bensen, T. Conrozier, D. Loeuille, A.J. Kivitz, D. Silver, B.E. Appleton, Intraarticular injection of anakinra in osteoarthritis of the knee: a multicenter, randomized, double-blind, placebo-controlled study, Arthritis Rheum. 61 (2009) 344–352. https://doi.org/10/bdfwpw.
[37] M. Kloppenburg, R. Ramonda, K. Bobacz, W.-Y. Kwok, D. Elewaut, T.W.J. Huizinga, F.P.B. Kroon, L. Punzi, J.S. Smolen, B.V. Cruyssen, R. Wolterbeek, G. Verbruggen, R. Wittoek, Etanercept in patients with inflammatory hand osteoarthritis (EHOA): a multicentre, randomised, double-blind, placebo-controlled trial, Annals of the Rheumatic Diseases. 77 (2018) 1757–1764. https://doi.org/10/gfrzrq.
[38] R.M. Fleischmann, H. Bliddal, F.J. Blanco, T.J. Schnitzer, C. Peterfy, S. Chen, L. Wang, S. Feng, P.G. Conaghan, F. Berenbaum, J. Pelletier, J. Martel-Pelletier, O. Vaeterlein, G.S. Kaeley, W. Liu, M.P. Kosloski, G. Levy, L. Zhang, J.K. Medema, M.C. Levesque, A Phase II Trial of Lutikizumab, an Anti–Interleukin-1α/β Dual Variable Domain Immunoglobulin, in Knee Osteoarthritis Patients With Synovitis, Arthritis Rheumatol. 71 (2019) 1056–1069. https://doi.org/10/ggcjn2.
[39] K.D. Ratanji, J.P. Derrick, R.J. Dearman, I. Kimber, Immunogenicity of therapeutic proteins: influence of aggregation, J Immunotoxicol. 11 (2014) 99–109. https://doi.org/10.3109/1547691X.2013.821564.
[40] A. Kuriakose, N. Chirmule, P. Nair, Immunogenicity of Biotherapeutics: Causes and Association with Posttranslational Modifications, J Immunol Res. 2016 (2016) 1298473. https://doi.org/10.1155/2016/1298473.
[41] M.F. Bachmann, R.M. Zinkernagel, Neutralizing antiviral B cell responses, Annu Rev Immunol. 15 (1997) 235–270. https://doi.org/10.1146/annurev.immunol.15.1.235.
[42] C. Babin, N. Majeau, D. Leclerc, Engineering of papaya mosaic virus (PapMV) nanoparticles with a CTL epitope derived from influenza NP, J Nanobiotechnology. 11 (2013) 10. https://doi.org/10.1186/1477-3155-11-10.
[43] A.A. Valiente-Gabioud, C. Veaute, M. Perrig, F.S. Galan-Romano, S.J. Sferco, I.S. Marcipar, Effect of repetitiveness on the immunogenicity and antigenicity of Trypanosoma cruzi FRA protein, Exp Parasitol. 127 (2011) 672–679. https://doi.org/10.1016/j.exppara.2010.11.011.
[44] M. Yagi, G. Bang, T. Tougan, N.M.Q. Palacpac, N. Arisue, T. Aoshi, Y. Matsumoto, K.J. Ishii, T.G. Egwang, P. Druilhe, T. Horii, Protective epitopes of the Plasmodium falciparum SERA5 malaria vaccine reside in intrinsically unstructured N-terminal repetitive sequences, PLoS One. 9 (2014) e98460. https://doi.org/10.1371/journal.pone.0098460.
[45] N. Hou, N. Jiang, Y. Ma, Y. Zou, X. Piao, S. Liu, Q. Chen, Low-Complexity Repetitive Epitopes of Plasmodium falciparum Are Decoys for Humoural Immune Responses, Front Immunol. 11 (2020) 610. https://doi.org/10.3389/fimmu.2020.00610.

[46] M. Krishna, S.G. Nadler, Immunogenicity to Biotherapeutics – The Role of Anti-drug Immune Complexes, Front Immunol. 7 (2016) 21. https://doi.org/10.3389/fimmu.2016.00021.

SUPPLEMENTARY INFORMATION

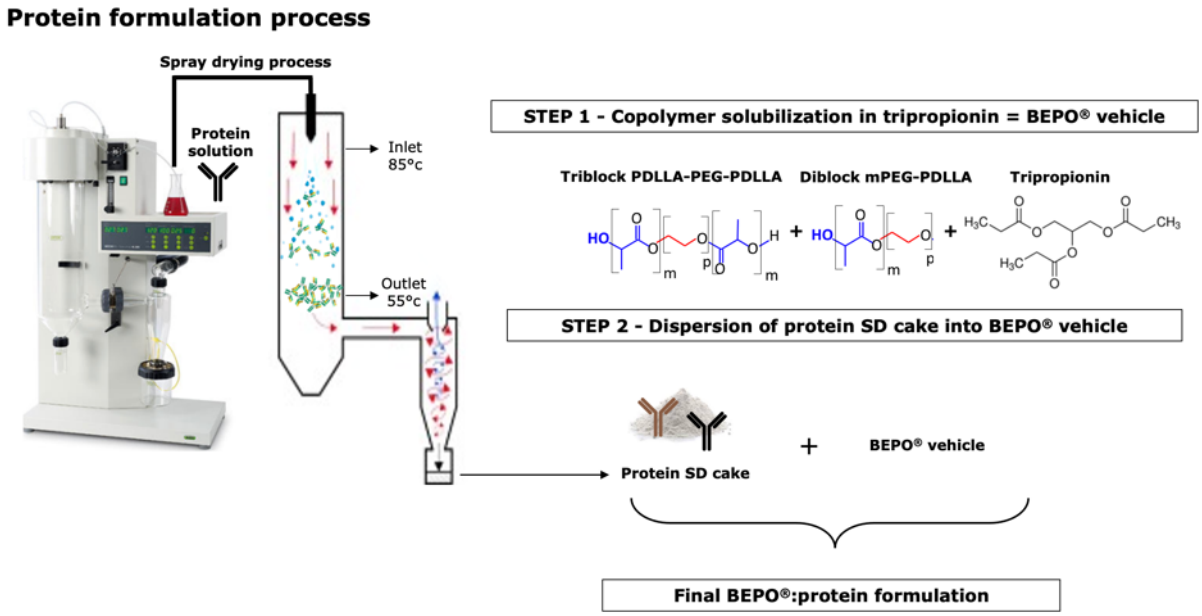

Supplementary figure S1: *Illustration of the protein formulation strategy using BEPO® copolymers.*

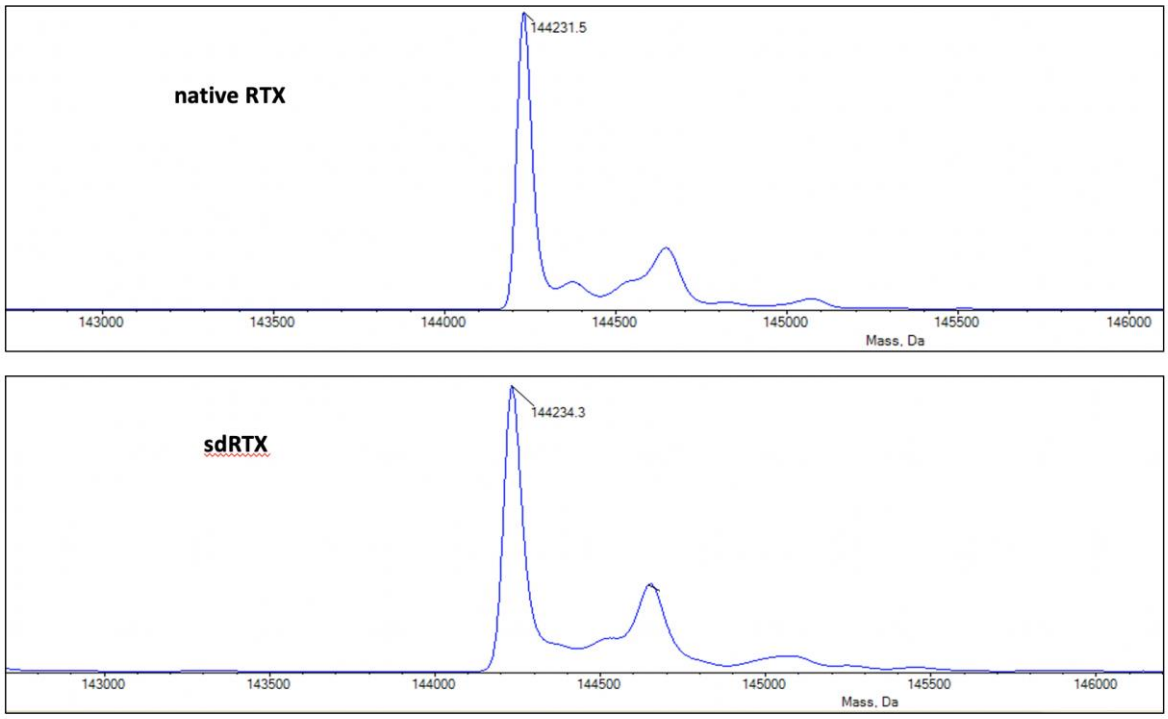

Supplementary figure S2: *Intact Mass (LC-MS) analysis performed after deglycosylation of the native RTX and sdRTX proteins.*

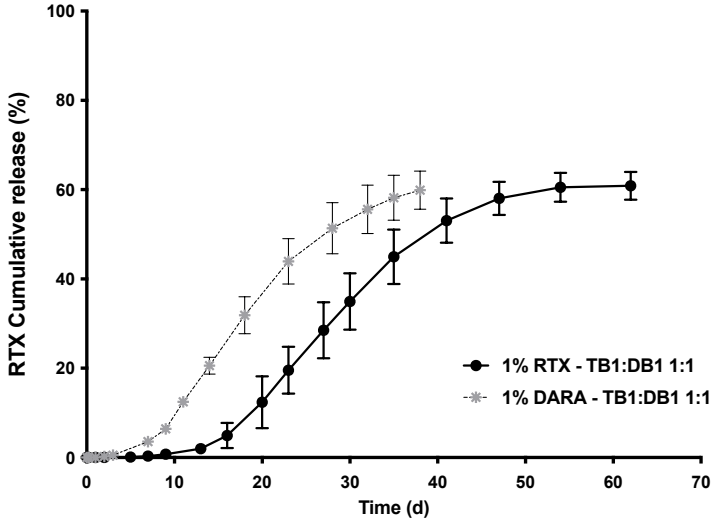

***Supplementary figure S3**: Comparison of the IVR profiles of spray dried RTX and DARA proteins formulated with V1 BEPO® vehicle (TB1:DB1 polymer composition).*

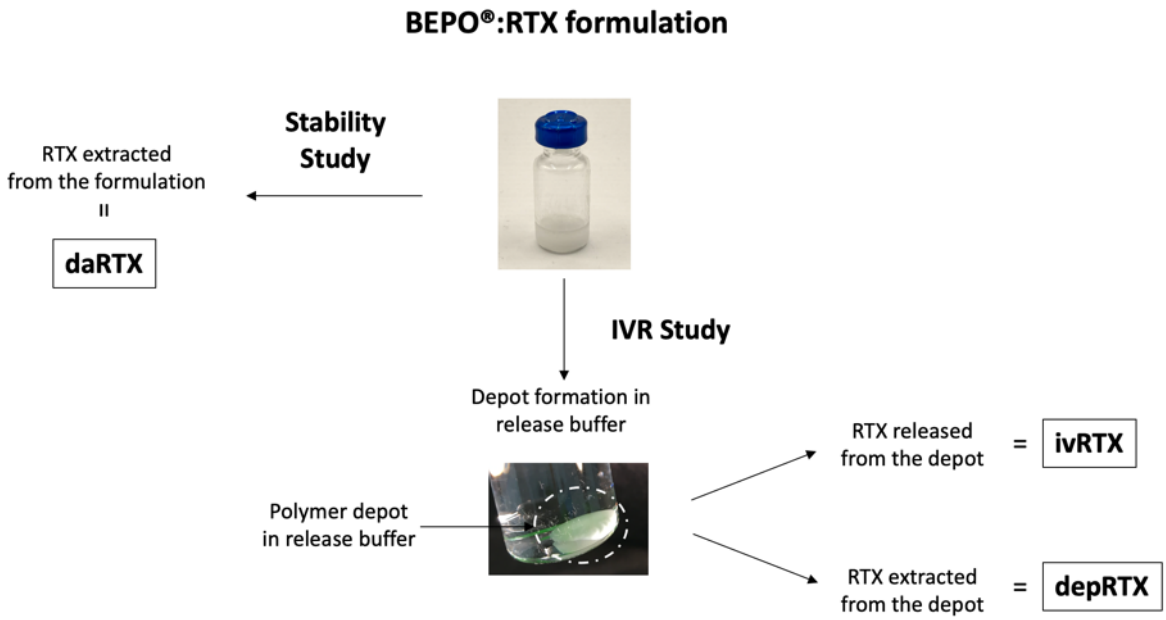

***Supplementary figure S4**: Illustration to define the nomenclature that was used to name RTX samples during the formulation process with BEPO® copolymers.*

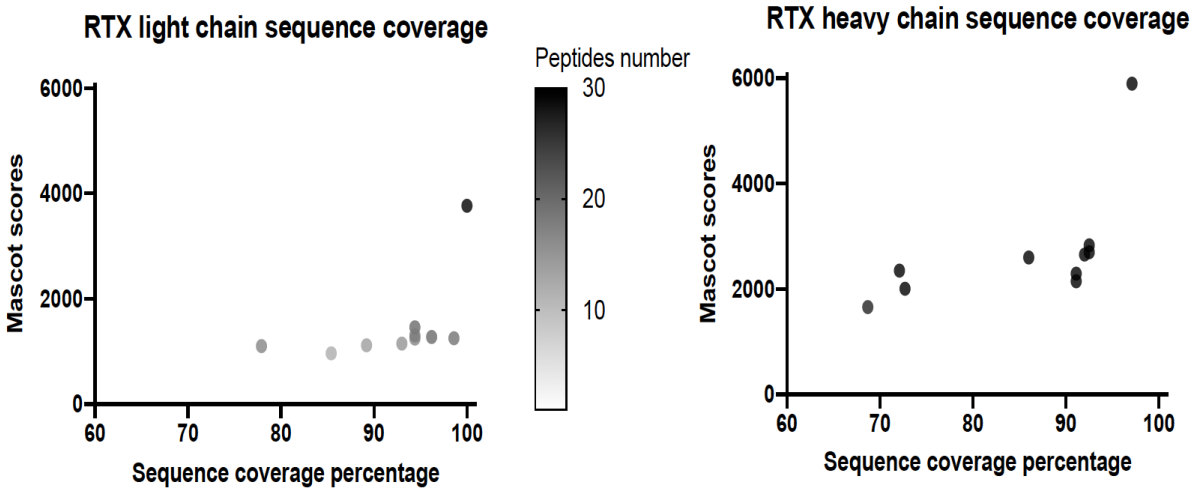

***Supplementary figure S5**: Amino acid sequence coverage determined by Q-tof Impact2 MS presented as function of percentage of sequence coverage (X axis), Mascot score (left axis) and peptide detected numbers (right colored axis). Light chain (left) and heavy chain (right) are presented separately. Each dot represents a formulated RTX sample (daRTX and ivRTX) taken at different time points. In both graphs, native RTX is the isolated dot in the top right corner.*

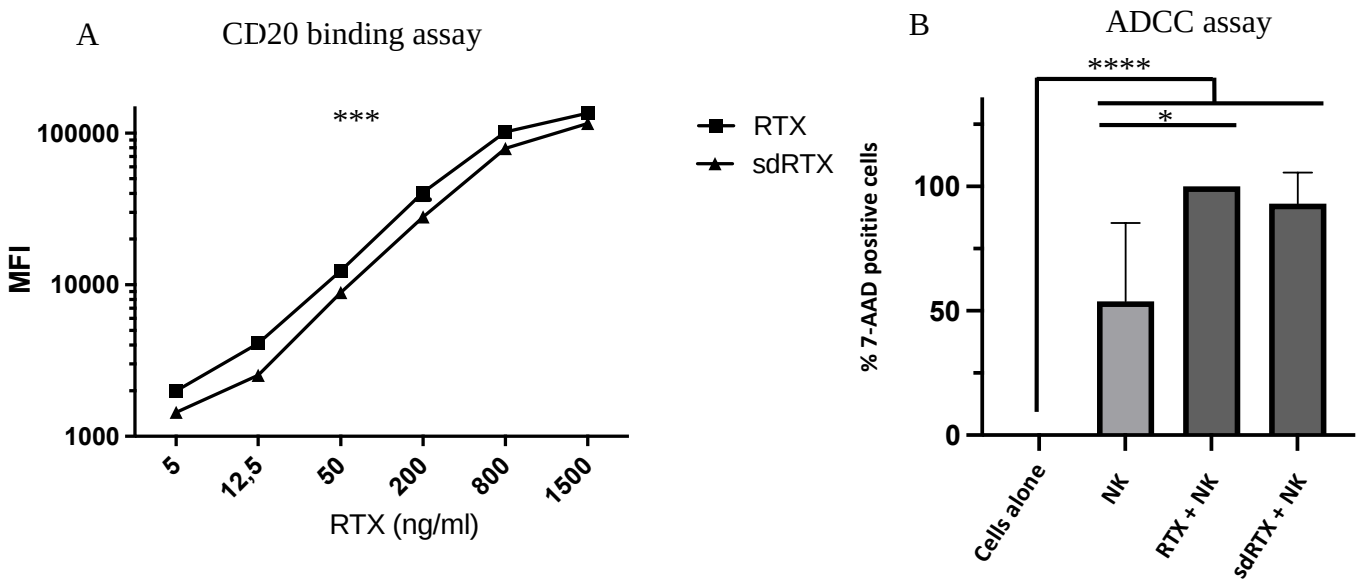

Supplementary figure S6*: Binding and ADCC assays carried out with sdRTX. (A) Binding to CD20 expressed by Raji cells. The depicted RTX samples were incubated for 30 min with Raji cells. RTX was revealed by an anti-human Fab-PE (1.875 µg/mL). The arithmetic mean fluorescence intensity (MFI) is represented. (B) ADCC on Raji cells. ADCC assay with RTX samples (10 µg/mL), in presence of NK cells (E:T, 3:1) was carried out overnight on Raji cells. Basal cell death was normalized to 0% and saline RTX+NK to 100%. Sample activity was presented as % of native RTX activity. Graph shows mean +/- SD of a minimum of two experiments performed in triplicate. Statistics in A are from spearman correlation over one experiment in triplicate ;***p<0,0009-0,0002; In B ADCC samples were compared by 2-ANOVA test, n = 5, *p< 0,030; **** p < 0.0001.*

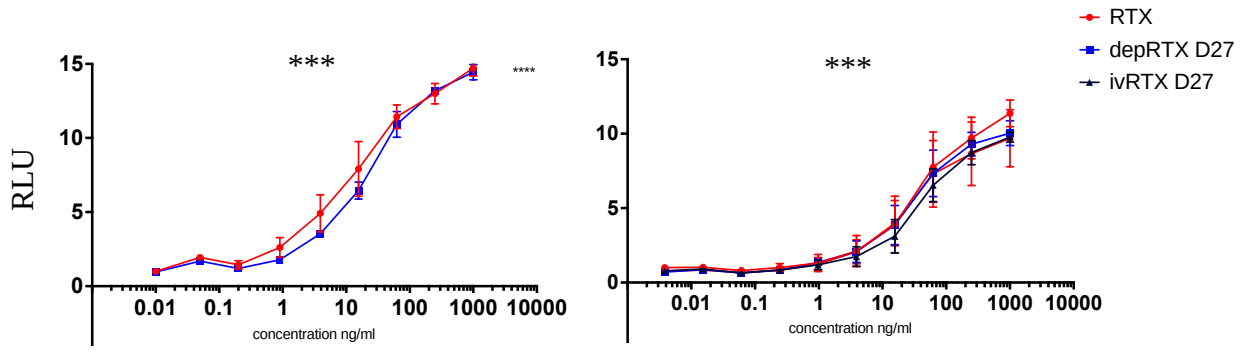

Supplementary figure S7: NFAT Reporter Activation Assay. *The capacity of formulated RTX samples to induce the NFAT signalling pathway in modified Jurkat cells was evaluated and compared to the one of native RTX. Signal is presented in Y-axis as relative luciferase units (RLU). Correlation was carried out by Spearman R test. Expressed as R square (0,903-1,000) and p-value ***; p<(0,0008-0,0001).*

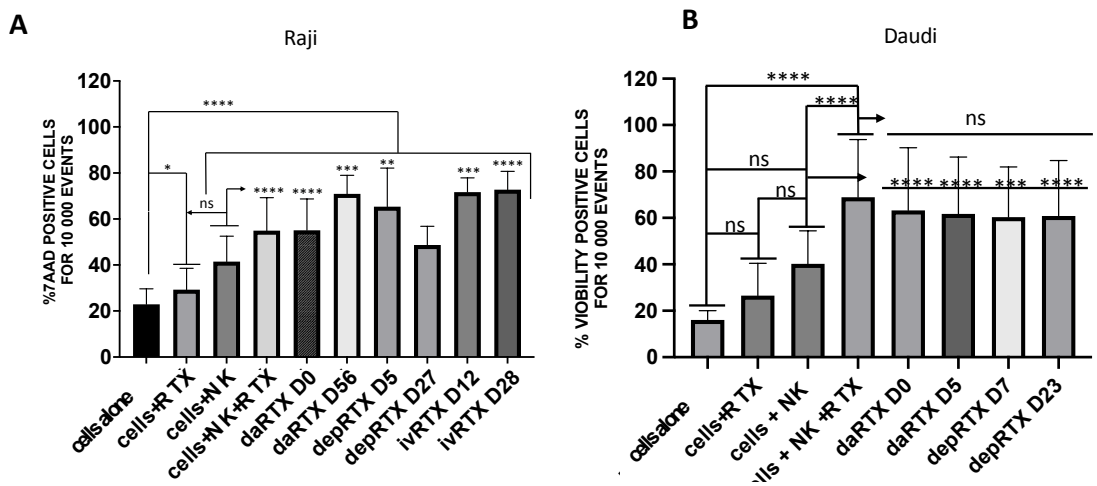

Supplementary figure S8: Functionality of formulated RTX. *All RTX samples were obtained from the F1 BEPO®:RTX and were either extracted from the formulation after storage at 4°C (daRTX samples) or obtained during the release study through the evaluation of the released protein (ivRTX) or the extraction of the protein from the solid polymer depot(depRTX). ADCC assay with the different RTX samples (10 µg/mL), in presence of NK cells (E:T, 3:1) was carried out overnight on Raji cells (7AAD stained) (A) or after 8 hours on Daudi cells (viobility stained) (B). Graphs show the mean +/- SD of a minimum of two experiments performed in triplicate. Samples were compared by 2-ANOVA test, n = 21, *p < 0.05, **p < 0.01, ***p=0.0001 and ****p<0.0001.*

Vehicle	TB:DB couple	Triblock	Diblock	Polymer content (% w/w)	TB:DB weight ratio
V1	TB1:DB1	3-9.8	1-6.5	20	1:1
V2	TB1:DB1	3-9.8	1-6.5	20	3:1
V3	TB1:DB2	3-9.8	2-27.8	20	1:1

Table 1 : *Composition of vehicles used to make BEPO®:protein formulations*

Proteins	CD16a K_D pH 7.4 (M)	CD16a V158F K_D pH 7.4 (M)	CD16b K_D pH 7.4 (M)	FcRn K_D pH 6.0 (M)
Native RTX	2.74×10^{-7}	9.52×10^{-7}	15.40×10^{-7}	2.73×10^{-8}
daRTX T0	1.30×10^{-7}	2.69×10^{-7}	4.97×10^{-7}	2.47×10^{-8}
daRTX 5w 4°C	1.13×10^{-7}	1.99×10^{-7}	5.72×10^{-7}	2.63×10^{-8}
depRTX 7d	1.00×10^{-7}	1.33×10^{-7}	2.96×10^{-7}	2.67×10^{-8}
depRTX 13d	0.92×10^{-7}	1.06×10^{-7}	2.19×10^{-7}	2.64×10^{-8}

***Table 2**: Affinity of formulated RTX samples for CD16a, CD16b and FcRn receptors*

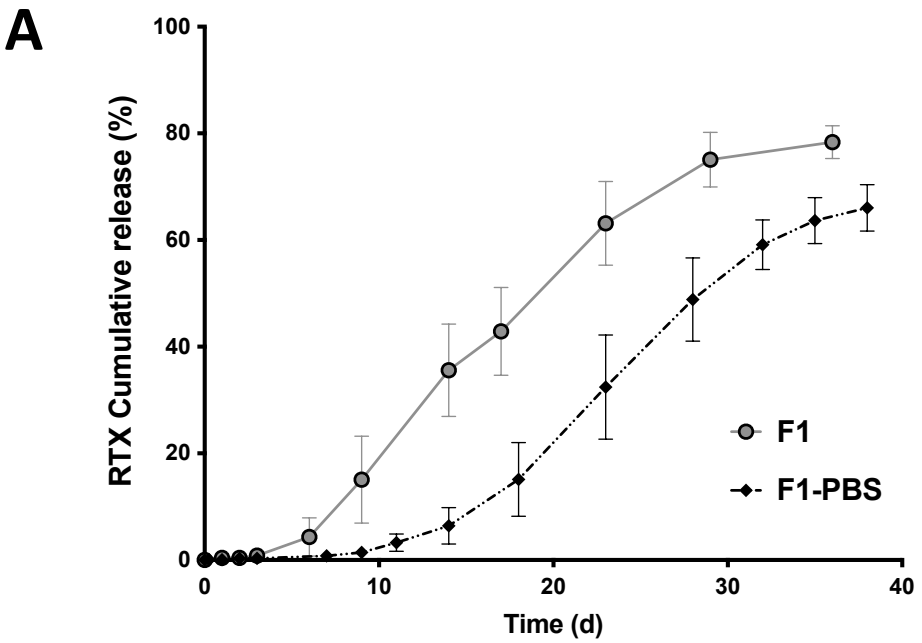

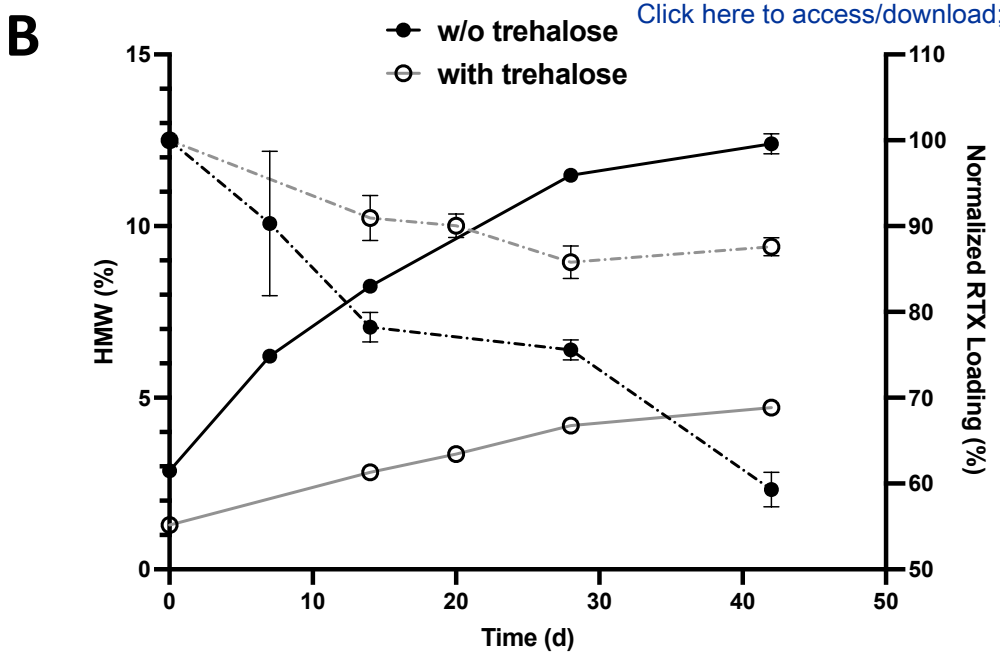

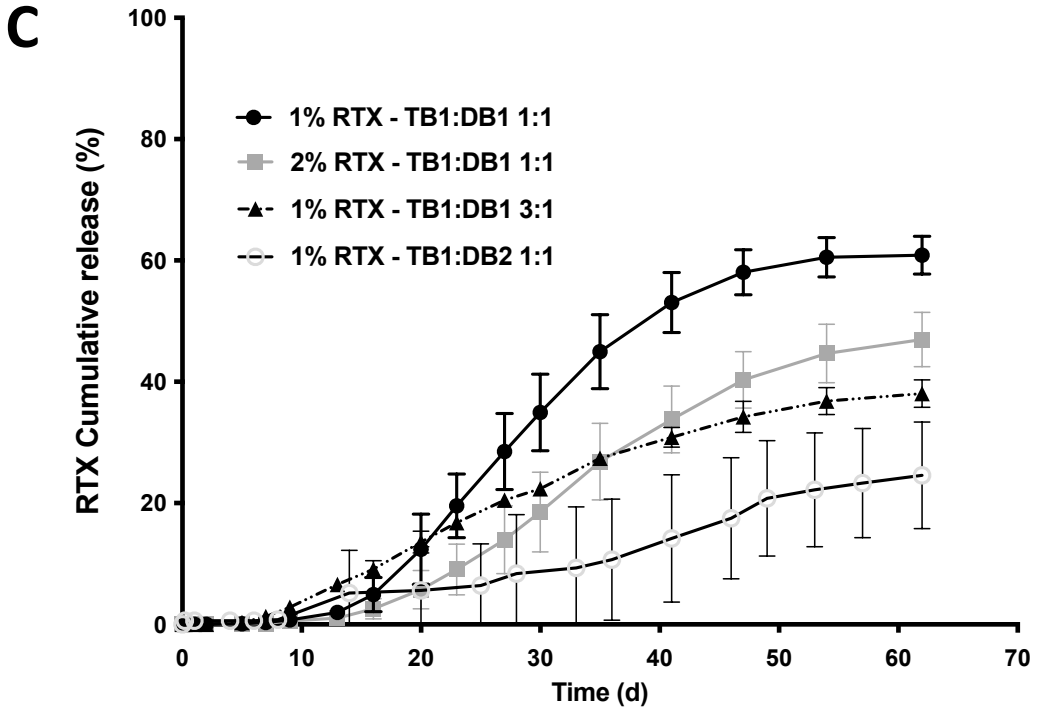

Fig. 2

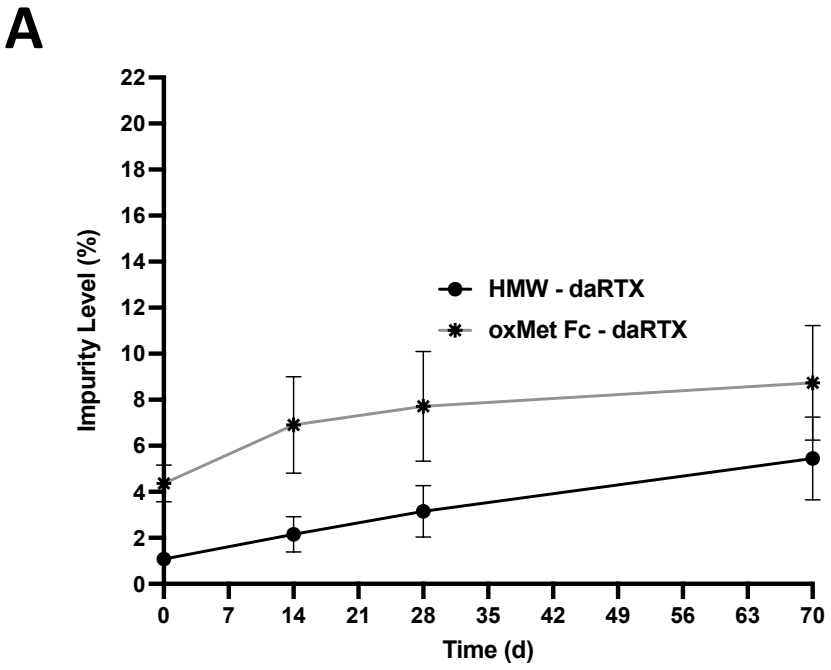

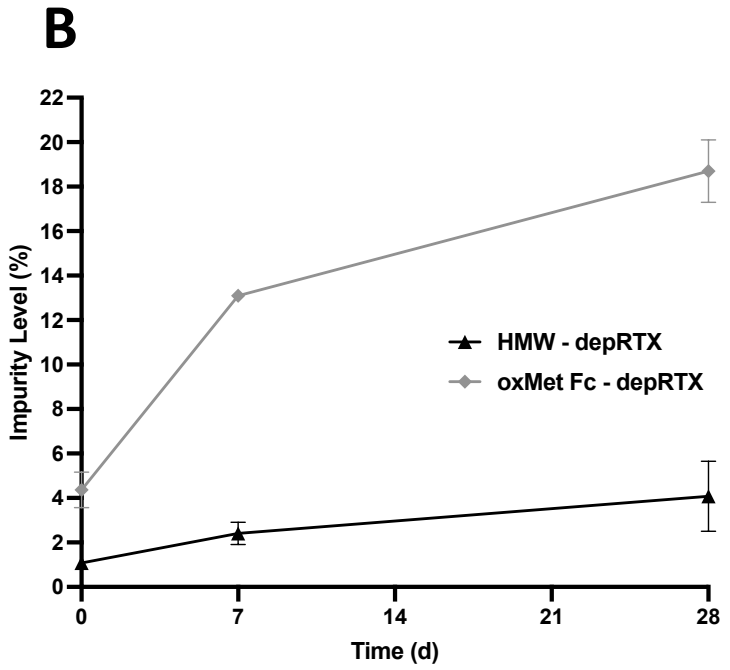

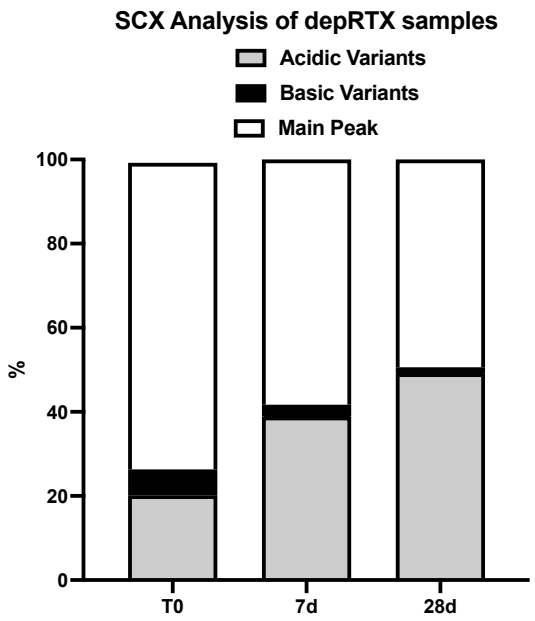

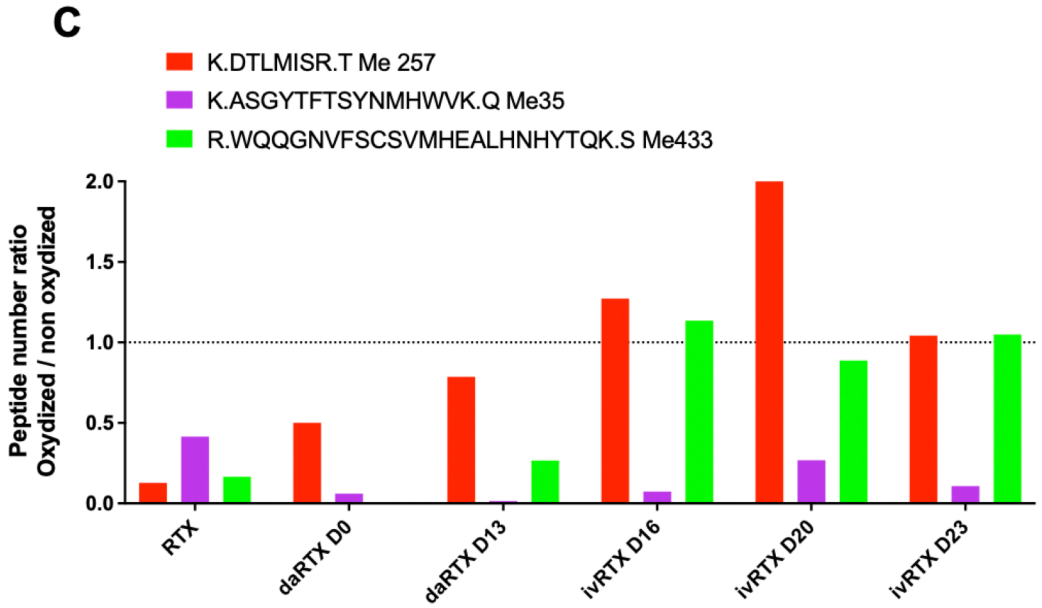

Fig. 3

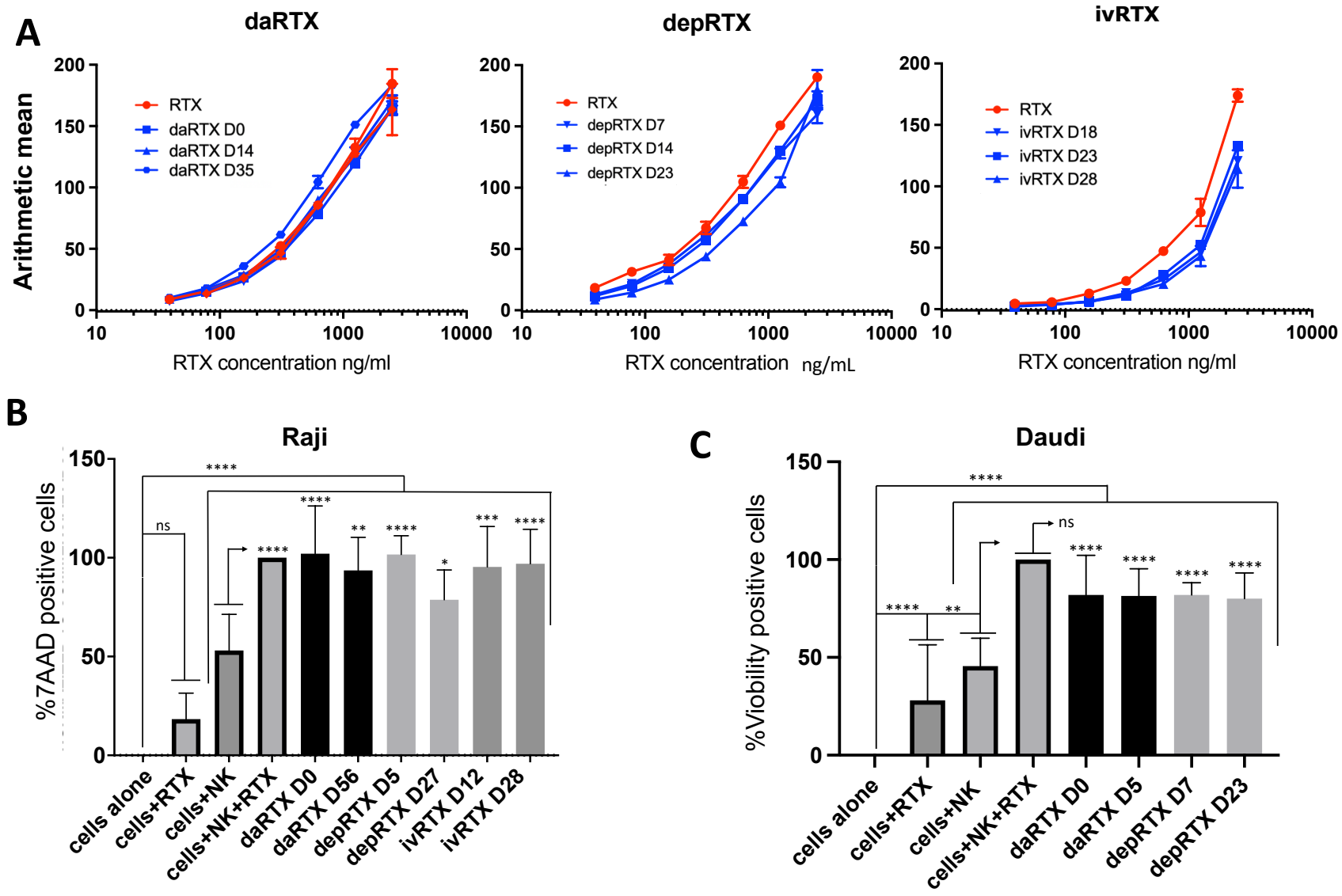

Fig. 4

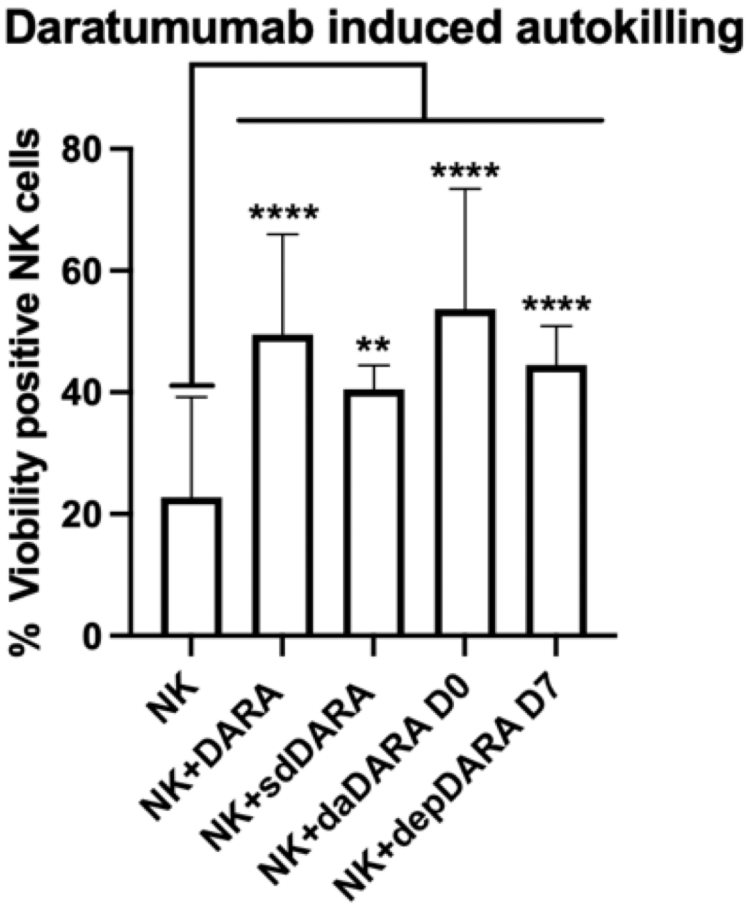

Fig. 5

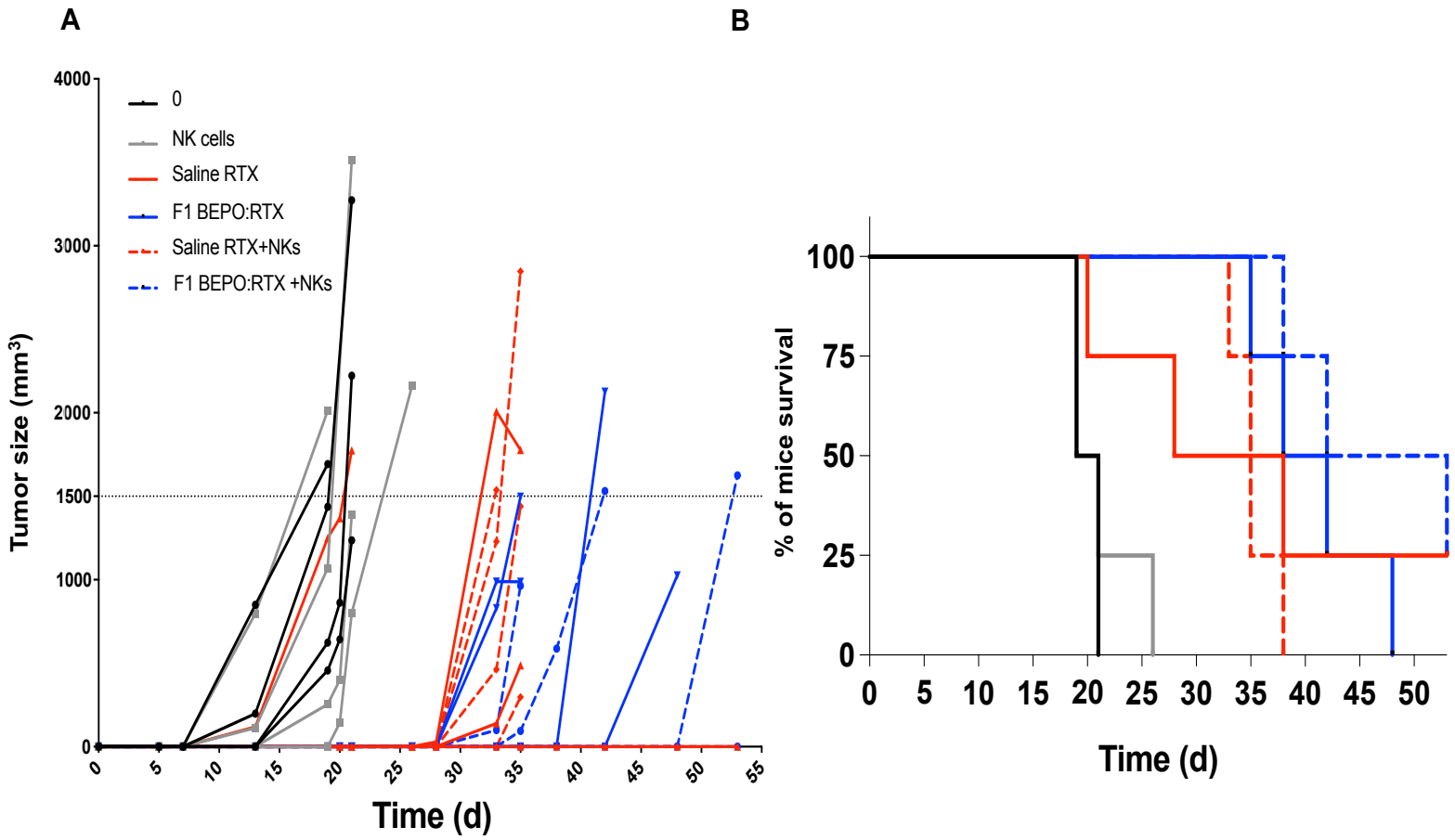

Fig. 6

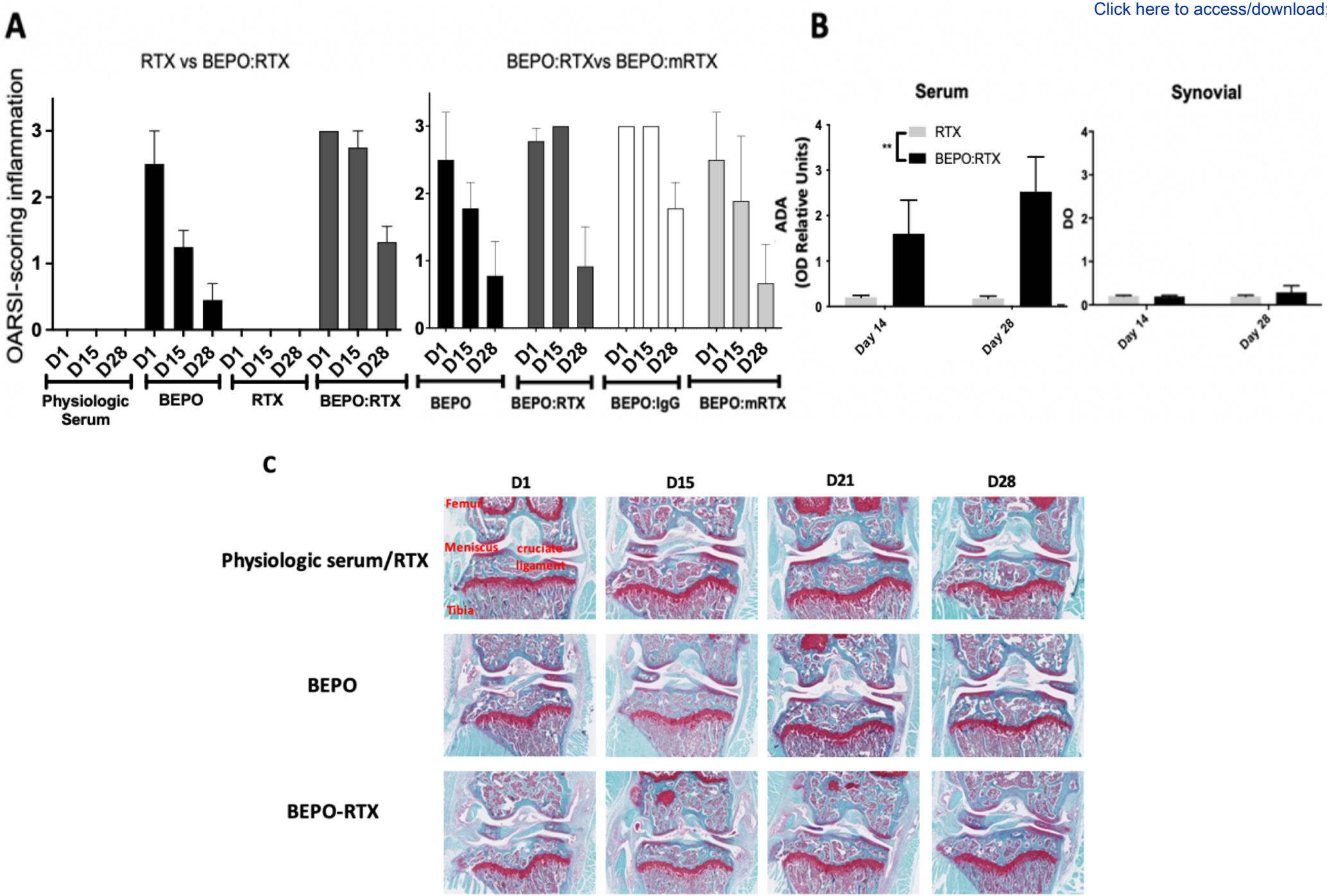

Fig. 7

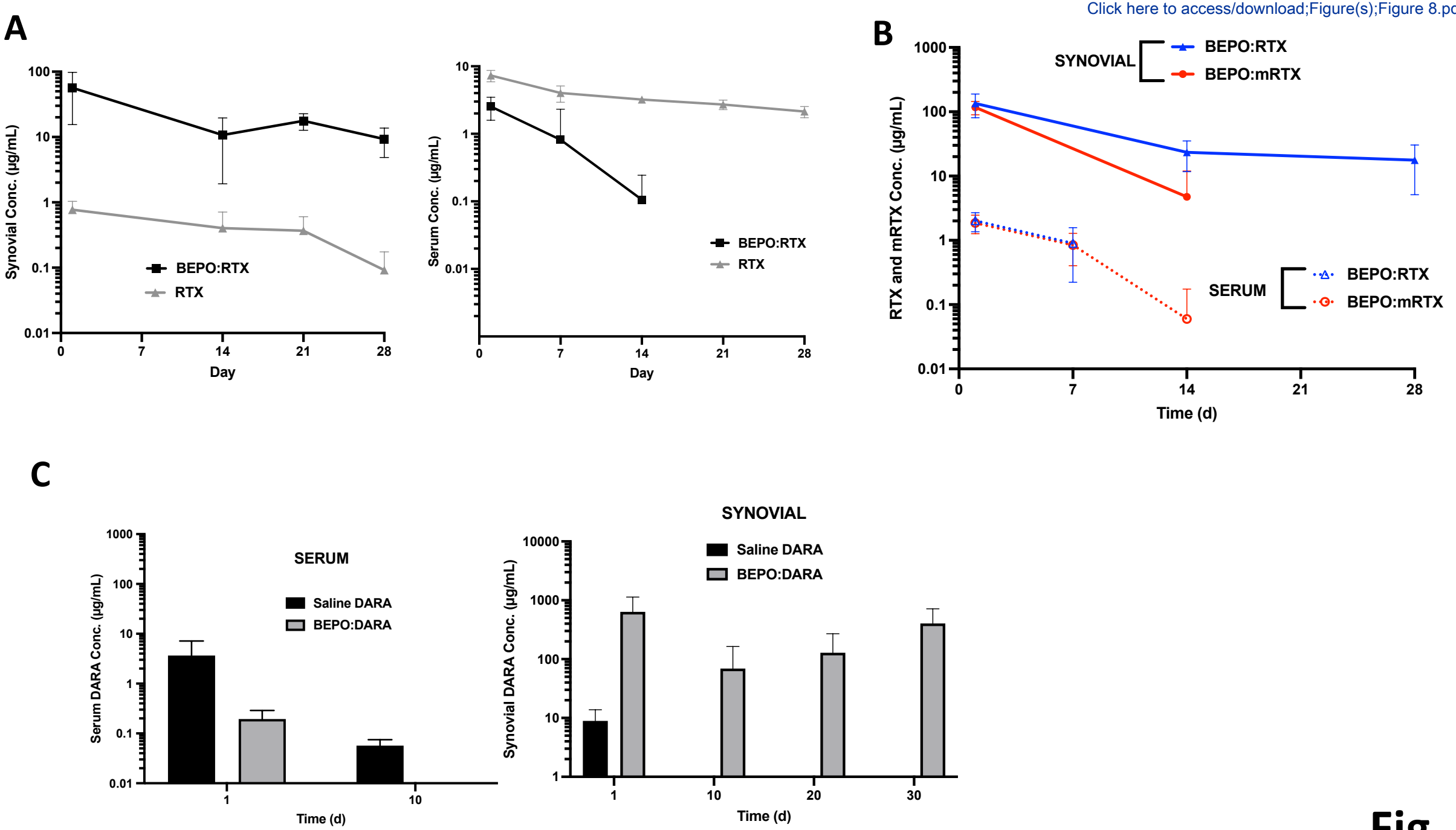

Fig. 8

Figure 1

A

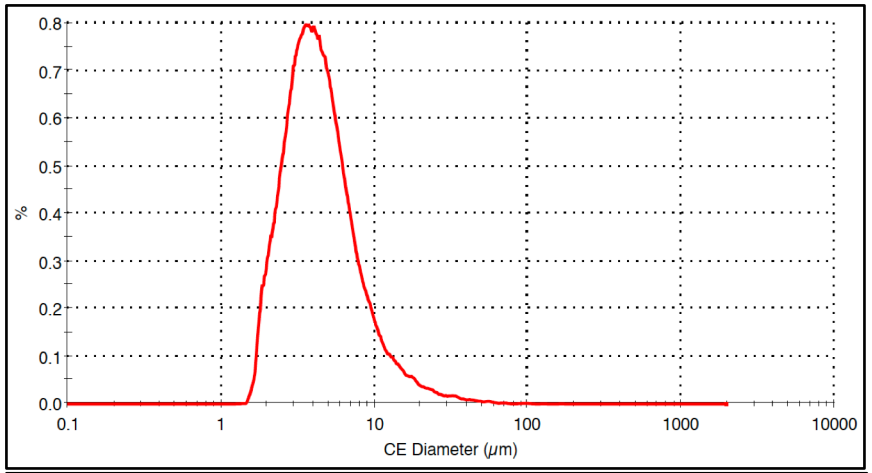

Result

CE Diameter Minimum (μm): 1.30	**CE Diameter D[n, 0.1] (μm):** 2.33
CE Diameter Maximum (μm): 195.19	**CE Diameter D[n, 0.5] (μm):** 4.14
CE Diameter Mean (μm): 5.46	**CE Diameter D[n, 0.9] (μm):** 9.05
CE Diameter STDV (μm): 5.25	**CE Diameter RSD (%):** 96.17

B

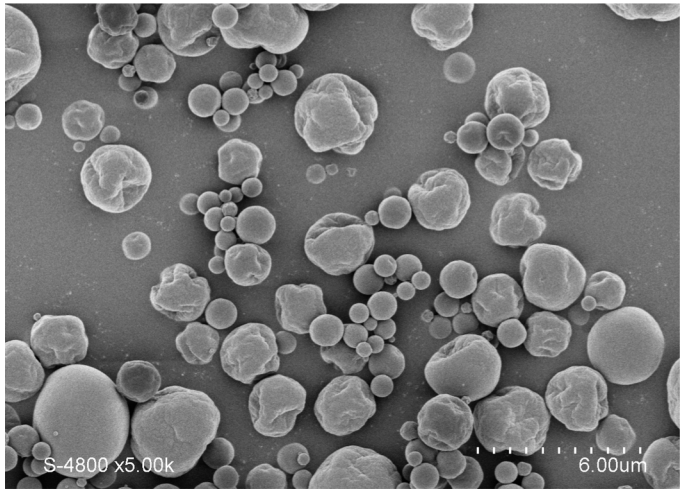

C

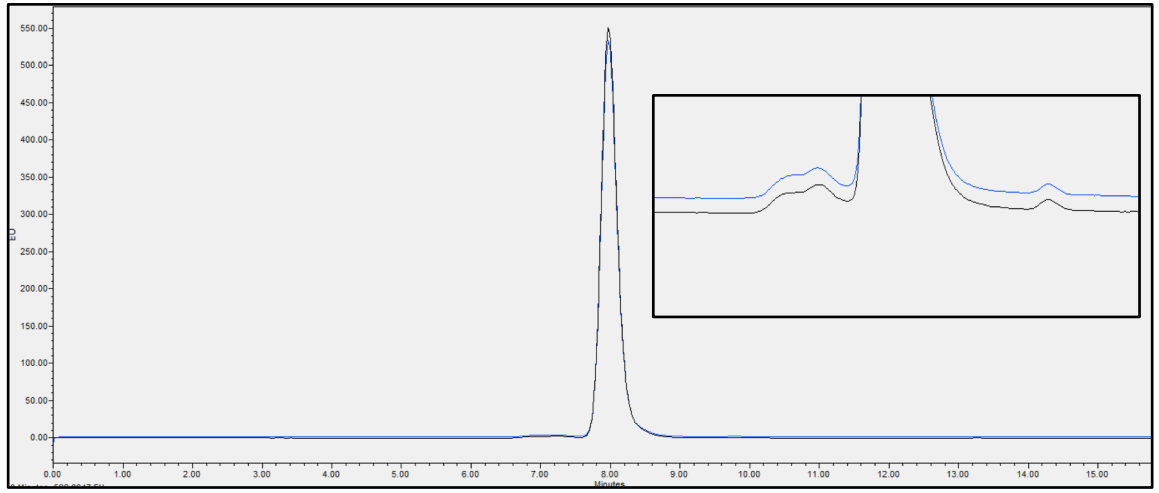

D

	T_i #1 (°C)	T_i #2 (°C)	T_i #3 (°C)
Native RTX	74.6	80.9	89.7
sdRTX	74.8	81.3	90.0

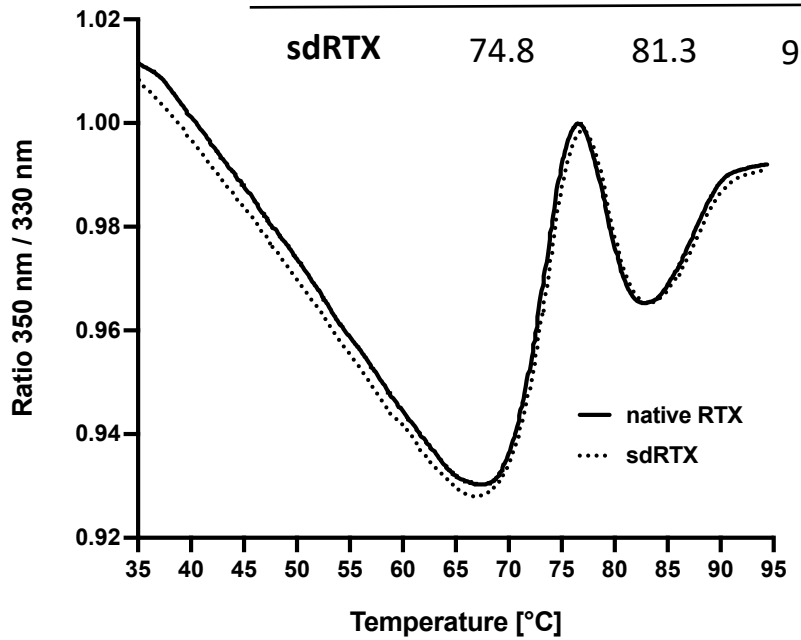

Fig. 1

Highlights

- Formulation of mAbs with an *in situ* forming depot technology using PEG-PLA copolymers.
- Formulated RTX showed full biological activity and minimal post-translational modifications.
- RTX formulation was as efficient as IV RTX treatment to inhibit *in vivo* tumor growth in NSG mice.
- mAbs formulations demonstrated superior PK properties after intra-articular delivery.

Author Contributions Statement

A.F., W.L., S.G., D.N., P.LP. and M.V. designed experiments. A.F., K.T. and S.G. performed experiments and analyzed results. A.F., M.V. and S.G. wrote the main manuscript text. All authors reviewed and approved the manuscript.